

Renormalization group evolution and power counting in nuclear matter

Manuel Pavon Valderrama^{1,*}

¹*School of Physics, Beihang University, Beijing 100191, China*

(Dated: March 23, 2026)

In nuclear matter, for interparticle separations larger than the healing distance (a characteristic long-distance scale of finite-density fermionic systems), the in-medium two-body wave function is essentially a free wave function. In terms of the renormalization group (RG), this implies that the running of the effective field theory (EFT) couplings freezes for r-space cutoffs above this distance (or p-space cutoffs below the corresponding healing momentum scale). As a consequence the leading order EFT description of nuclear matter (understood here as the infrared limit of the RG) corresponds to the mean-field approximation and a set of tree-level (i.e. perturbative) leading contact-range couplings. Though the contacts do in principle inherit the power counting they had in the vacuum, their iteration is suppressed in the infrared, explaining why they become perturbative in nuclear matter. In addition to the contact-range potential, RG evolution requires the inclusion of density-dependent terms in the equation of state that can be represented by a pseudo-potential, which (unlike the genuine contacts) should not be iterated. The LO EFT description ends up being a subset of Skyrme forces previously identified by the Orsay group.

I. INTRODUCTION

Effective field theories (EFTs) are model independent and systematically improvable descriptions of low energy phenomena [1]. They are ideally suited for situations in which a more fundamental, high energy description is unavailable or simply impractical. The fundamental theory of strong interactions is quantum chromodynamics (QCD), which owing to asymptotic freedom is not analytically solvable at the characteristic low momenta of nucleons within nuclei. EFTs are the natural answer to this limitation [2–6], which otherwise can only be overcome by brute force, i.e., lattice QCD [7, 8]. In addition, they are able to bridge the gap between QCD and nuclear physics thanks to the fact that EFTs can be understood as the infrared renormalization group (RG) evolution of their underlying theory (QCD in this case).

This connection is well-understood regarding the derivation of nuclear forces, where the EFT potential takes the form of a power series in terms of the small ratio Q/M :

$$V_{\text{EFT}} = \sum_{\nu} V^{(\nu)} \left(\frac{Q}{M} \right)^{\nu}, \quad (1)$$

with Q and M referring, respectively, to the low- and high-energy scales of the theory. In nuclear physics Q might represent the pion mass m_{π} or the momentum exchanged by the nucleons $|\vec{q}|$, while M refers to the rho or nucleon masses, m_{ρ} or m_N . The set of rules by which this expansion is structured is the power counting of the EFT, which is in turn intimately intertwined with its infrared RG flow [9, 10].

The extension of the EFT description to finite nuclei and infinite nuclear matter is conceptually straightforward, but often unachievable in practice. While in

principle it merely entails the direct calculation of nuclear properties from few-nucleon forces, the limitation remains that this type of ab-initio approach is only computationally viable for light- and medium-mass nuclei.

Heavy-mass nuclei and nuclear matter are often described instead in terms of effective interactions (effective, that is, in the phenomenological sense) such as Skyrme [11] or Gogny [12]. However, they often lack a clear connection to an underlying Hamiltonian or Lagrangian formulation [13–15], which prevents us from deriving them within the EFT frameworks used to describe few-nucleon systems. In principle, these systems are still suspected to be amenable to an EFT description of their own — energy density functionals (EDFs) and the aforementioned phenomenological effective interactions do have a strong EFT resemblance or flavor [16–18], so to speak —, though current efforts to formulate a rigorous EFT for EDFs remain incomplete despite ongoing efforts [19–29].

Here I will consider the RG evolution of EFT contact-range interactions in nuclear matter. The key idea is the identification of the healing distance [30–33] as the relevant scale for defining the infrared limit of strongly interacting systems of fermions at finite density. This is the distance above which the two-nucleon wave function in the medium essentially becomes a plane wave. It is a consequence of the Pauli exclusion principle, which strongly suppresses scattering between nucleon pairs in the Fermi sea, resulting in a free wave function (modulo small oscillatory corrections) for momenta below the Fermi momentum. The RG evolution of the contact-range couplings depends on the form of the wave function (as explicitly shown in [34]), where for a free wave function the couplings are approximately scale independent. That is, the RG flow of the couplings basically freezes at scales softer than the healing distance, while at harder scales it will be given by two-body correlations (i.e. the in-medium two-body wave function) and reproduce the vacuum RG flow. Moreover, as is well-known, the in-medium two-

* mpavon@buaa.edu.cn

body phase shifts become zero [32], i.e., in-medium two-body scattering is trivial.

In terms of the RG and its infrared evolution, the previous observation suggests the formulation of a *perturbative* low energy EFT for nuclear matter. It is perturbative in the sense that interactions are not to be iterated at all orders (as implied by the triviality of in-medium two-body scattering), despite the fact that the size of said interactions is still infrared-enhanced. This non-perturbative to perturbative transition is not trivial to prove though. The lowest order of this EFT corresponds to the mean-field (MF) approximation, in which couplings are approximately scale independent, while the vacuum running of these couplings at harder scales is recovered order-by-order with beyond-mean-field (BMF) corrections. This second observation defines the conditions by which the low energy description of nuclear matter can be connected with that of few-nucleon forces (in particular, their contact-range components).

The manuscript is structured as follows: in Section II I illustrate with the concrete example of a contact-range theory the appearance of the healing distance, how it leads to the freeze of the RG evolution of the couplings and how loop corrections become perturbative. In Section III I analyze the power counting of contact-range two-body forces in nuclear matter, and briefly discuss the role of pion exchanges and few-body forces. Section IV deals with the appearance of density-dependent contributions to the energy per nucleon that originate specifically from the infrared RG evolution in nuclear matter. Finally, in Section V I summarize and discuss the main findings of the present work. Appendices A, B and C include technical details or in-depth discussions of the G-matrix, the calculation of loop corrections in nuclear matter and power counting, respectively.

II. THE HEALING DISTANCE AND THE RENORMALIZATION GROUP FLOW

One interesting characteristic of infinite fermion systems is that the two-body wave function quickly approaches the free wave function at large interparticle distances. As a consequence of the exclusion principle, the fermions below the Fermi momentum (i.e., at low energies) are prevented from scattering with each other and thus end up behaving as free particles [32].

In nuclear physics this is referred to as the healing of the wave function [33]. From the EFT perspective, this has very interesting consequences because the running of the contact-range couplings can be determined from the behavior of the wave function at different distances or momenta [34]. For a perturbative contact-range coupling, its running is determined by

$$\frac{d}{d\Lambda} \left[C(\Lambda) \langle \Psi_{\text{EFT}} | \mathcal{O}_C | \Psi_{\text{EFT}} \rangle \right] = 0, \quad (2)$$

where Ψ_{EFT} is the EFT wave function, Λ the cutoff, \mathcal{O}_C

a contact-range operator (i.e. a regularized Dirac-delta) and $C(\Lambda)$ the coupling. If Ψ_{EFT} is a free wave function, the RG equation simplifies to

$$\frac{d}{d\Lambda} C(\Lambda) = 0, \quad (3)$$

which implies that the coupling does not run. This happens independently of whether one originally relies on perturbative or non-perturbative arguments, though if the two-body wave function is well approximated by a plane wave at large distances is because the contact-range interaction is indeed perturbative at low energies.

For nuclear matter the previous argument implies that the evolution of the coupling constants approximately freezes for cutoffs softer than the healing distance. Thus the infrared limit of the RG equations results in couplings that eventually become independent of the cutoff, that is

$$C(\Lambda < \Lambda^*) \approx C(\Lambda^*), \quad (4)$$

where Λ^* is a momentum scale that is related to the healing distance or the Fermi momentum. If non-running couplings are indeed perturbative (independently of the reason why they do not run), this leads to a very convenient and simple EFT description of nuclear matter in which the contact-range interactions are perturbative (regardless of whether this is the case in the vacuum) and their size given by the new momentum scale Λ^* . Incidentally, this is how Skyrme interactions work (for which calculations are usually done at tree level).

It is interesting to notice that if one is using the MF approximation, the two-body wave function is indeed a free wave function. That is, in this approximation the coupling constants do not run and are cutoff independent instead. This also implies that if one wants to recover in the medium the ultraviolet running of the coupling constants in the vacuum (i.e. the running for $\Lambda > \Lambda^*$) it will be necessary to include BMF corrections so as to reproduce the two-body short-range correlations on which the ultraviolet running depends.

The practical consequence of this observation is that if one wants to connect the EFT description of few-nucleon systems in the vacuum with that of extended systems, such as nuclear matter or heavy nuclei, then it is necessary to concentrate on soft cutoffs. Descriptions with hard cutoffs instead require BMF corrections in order to recover (in the form of an expansion if MF is the starting point) the renormalizability properties of the EFT in the vacuum.

The rest of this section explains in more detail the healing of the wave function and how it explicitly affects the running of the coupling constant. For this, (i) the vacuum and in-medium two-body wave functions are compared, (ii) a cutoff is introduced and from it the running of the lowest order coupling constant is calculated and (iii) the power counting of this coupling, in particular whether it is perturbative or not, is discussed. Basically, I will be giving a more detailed derivation of the physical intu-

itions discussed in the previous paragraphs. The formalism relies on the r-space representation of the Lippmann-Schwinger and Bethe-Goldstone equations. Not every EFT practitioner is familiar with this choice, though this is not a problem: the arguments about power counting will be derived again in Section III in a more usual language. Further details about the calculations appearing in the present Section are provided in Appendix A.

A. The two-body wave function

In the vacuum, the zero-energy S-wave wave function of a two-body system with a zero-range interaction is given by the well-known expression

$$\Psi_0(\vec{r}) = \frac{1}{\sqrt{4\pi}} \frac{u_0(r)}{r} \propto \left(1 - \frac{a_0}{r}\right), \quad (5)$$

where a_0 is the scattering length. The intention here is to compare this wave function with the corresponding one for a two-fermion system below the Fermi sea. Even though in this latter case analytic expressions are known (actually for a hard core [35, 36] or a delta-shell [37], though they are easily extended to the zero-range case), it would be convenient nonetheless to explain how the in-medium wave function is obtained. This will prove useful for calculating the finite cutoff version of this wave function and the running of the coupling constant at finite densities.

For deriving the in-medium two-body wave function it will be convenient to consider first the following r-space version of the Lippmann-Schwinger equation for the vacuum case

$$\Psi_{\vec{p}}(\vec{r}) = e^{i\vec{p}\cdot\vec{r}} + \int d^3\vec{r}' G_0(\vec{r} - \vec{r}') V(\vec{r}') \Psi_{\vec{p}}(\vec{r}'), \quad (6)$$

in which \vec{p} is the center-of-mass momentum of the two-body system and V the two-body potential (which is zero-range in the case at hand). The propagator G_0 reads

$$\begin{aligned} G_0(\vec{r} - \vec{r}') &= m_N \int \frac{d^3\vec{k}}{(2\pi)^3} \frac{e^{i\vec{k}\cdot(\vec{r}-\vec{r}')}}{p^2 + i\epsilon - k^2} \\ &= -\frac{m_N}{4\pi} \frac{e^{ip|\vec{r}-\vec{r}'|}}{|\vec{r} - \vec{r}'|}, \end{aligned} \quad (7)$$

and represents the propagation of the two particles within a loop, where m_N is the nucleon mass as I am assuming the particles to be nucleons. Within this formalism there is a well-known extension for two fermions interacting within the Fermi sea — the Bethe-Goldstone equation (check [38] for a review) — which in r-space reads

$$\Psi_{\vec{p},\vec{P}}(\vec{r}) = e^{i\vec{p}\cdot\vec{r}} + \int d^3\vec{r}' K_0(\vec{r} - \vec{r}') V(\vec{r}') \Psi_{\vec{p},\vec{P}}(\vec{r}'), \quad (8)$$

where the two-body wave function now depends not only on the relative momentum $\vec{p} = (\vec{p}_1 - \vec{p}_2)/2$ but also on the total momentum $\vec{P} = \vec{p}_1 + \vec{p}_2$ (with \vec{p}_1 and \vec{p}_2 the momenta of particles 1 and 2). In this expression K_0 is the in-medium two-body propagator, which reads

$$\begin{aligned} K_0(\vec{r} - \vec{r}') &= \\ m_N \int \frac{d^3\vec{k}}{(2\pi)^3} \frac{e^{i\vec{k}\cdot(\vec{r}-\vec{r}')}}{p^2 - k^2} \theta(k_1 - k_F) \theta(k_2 - k_F), \end{aligned} \quad (9)$$

where k_F is the Fermi momentum and with k_1, k_2 the magnitude of the momenta of the two particles within the loop:

$$k_1 = \left|\frac{\vec{P}}{2} + \vec{k}\right| \quad \text{and} \quad k_2 = \left|\frac{\vec{P}}{2} - \vec{k}\right|. \quad (10)$$

That is, K_0 simply represents G_0 when rescattering is limited to two-body states that are not within the Fermi sea (where this explains why the in-medium two-body wave function depends both on \vec{p} and \vec{P}).

If one particularizes the previous expressions for a zero-range interaction and for $\vec{p} = 0$ and $\vec{P} = 0$, one obtains

$$\Psi_0(\vec{r}) = 1 + \lambda G_0(r), \quad (11)$$

$$\Psi_{0,0}(\vec{r}) = 1 + \mu K_0(r), \quad (12)$$

with λ and μ being proportionality constants, and G_0 and K_0 the evaluation of the vacuum and in-medium propagators for zero external momenta:

$$\begin{aligned} G_0(r) &= -m_N \int \frac{d^3\vec{k}}{(2\pi)^3} \frac{e^{i\vec{k}\cdot\vec{r}}}{k^2} \\ &= -\frac{m_N}{4\pi} \frac{1}{r}, \end{aligned} \quad (13)$$

$$\begin{aligned} K_0(r) &= -m_N \int \frac{d^3\vec{k}}{(2\pi)^3} \frac{e^{i\vec{k}\cdot\vec{r}}}{k^2} \theta(k - k_F) \\ &= -\frac{m_N}{4\pi} \left[\frac{1}{r} - \frac{2}{\pi} \frac{\text{Si}(k_F r)}{r} \right], \end{aligned} \quad (14)$$

where $\text{Si}(x)$ is the sine-integral function:

$$\text{Si}(x) = \int_0^x \frac{\sin t}{t} dt. \quad (15)$$

The proportionality constants can be determined from a comparison with the equations

$$|\Psi_{\vec{p}}\rangle = |\vec{p}\rangle + \frac{1}{E - H_0} T(E) |\vec{p}\rangle, \quad (16)$$

$$|\Psi_{\vec{p},\vec{P}}\rangle = |\vec{p}\rangle + \frac{Q_F}{E - H_0} G(E) |\vec{p}\rangle, \quad (17)$$

where $T(E)$ and $G(E)$ are the T- and G-matrices, and with Q_F the projector that removes intermediate states within the Fermi sea. After Fourier-transforming into r-space and taking the limit of zero external momenta, one

ends up with the identification of λ and μ with $T(E)$ and $G(E)$, respectively, where

$$T(E \rightarrow 0) \rightarrow \frac{4\pi}{m_N} a_0, \quad (18)$$

$$G(E \rightarrow 0) \rightarrow \frac{4\pi}{m_N} \frac{1}{\frac{1}{a_0} - \frac{2}{\pi} k_F}, \quad (19)$$

with $E = p^2/m_N$ the center-of-mass energy of the two-body system. For the G-matrix the $P \rightarrow 0$ limit has been implicitly understood, where a more detailed derivation of this limit can be found in Appendix A.

Putting the pieces together, the zero-energy two-body wave function in the medium reads

$$\Psi_{0,0}(\vec{r}) = 1 - \frac{1}{\frac{1}{a_0} - \frac{2}{\pi} k_F} \left[\frac{1}{r} - \frac{2}{\pi} \frac{\text{Si}(k_F r)}{r} \right]. \quad (20)$$

The vacuum solution is reproduced as the $k_F \rightarrow 0$ limit of the in-medium wave function. In Fig. 1 a comparison of the vacuum and in-medium solutions for $a_0 = -23.7$ fm — corresponding to the 1S_0 scattering length in the two-nucleon system — and $k_F = 1.33$ fm (i.e. the Fermi momentum of the saturation density of nuclear matter) is shown. There one can clearly see how the in-medium wave function becomes approximately constant for $k_F r \geq 1$, modulo decreasing oscillations.

The oscillations are a well-known part of the asymptotic ($k_F r \gg 1$) behavior of the wave function:

$$\begin{aligned} \Psi_{0,0}(\vec{r}) \rightarrow 1 - \frac{\frac{2}{\pi} k_F}{\frac{1}{a_0} - \frac{2}{\pi} k_F} \left[\frac{\cos(k_F r)}{(k_F r)^2} + \frac{\sin(k_F r)}{(k_F r)^3} \right] \\ + \mathcal{O}\left(\frac{1}{r^4}\right), \end{aligned} \quad (21)$$

where it can be appreciated the pattern of $1/r^2$ and $1/r^3$ corrections over the free solution [38]. It is interesting to notice the absence of a $1/r$ component, which is related to scattering. This reflects the well-known fact that the in-medium phase shifts are zero. These oscillations are faintly visible in Fig. 1.

B. In-medium renormalization group flow

As is well known, the form of the two-body wave function contains in itself interesting information about the renormalization of the two-body system at low energies. In particular, by introducing a cutoff it will be possible to analyze the RG evolution of the contact-range couplings, determine their sizes in the infrared limit and hence their power counting. Of course, this is also the case at finite densities.

One might include a cutoff R_c by regularizing the contact-range potential as a delta-shell at the radius $r = R_c$:

$$V_C(r; R_c) = C_0(R_c) \frac{\delta(r - R_c)}{4\pi R_c^2}, \quad (22)$$

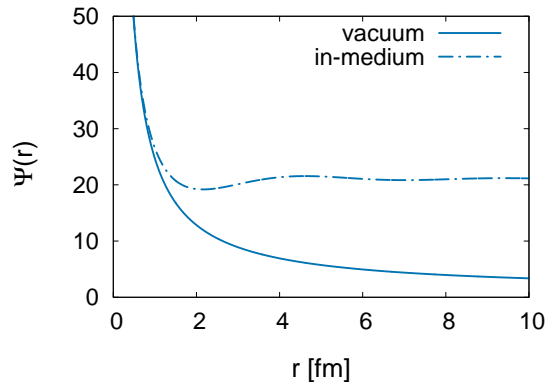


FIG. 1. Vacuum and in-medium zero-energy, S-wave two-body wave functions. The normalization has been set from the condition that both wave functions coincide in the $r \rightarrow 0$ limit, where $\Psi(r) \rightarrow (1 - a_0/r)$ with a_0 the scattering length. With this normalization in the asymptotic $r \rightarrow \infty$ limit the wave function approaches $\Psi \rightarrow 1$ in vacuum and $\Psi \rightarrow (1 - 2a_0 k_F/\pi)$ in medium. The scattering length and Fermi momentum have been taken to be $a_0 = -23.7$ fm and $k_F = 1.33$ fm $^{-1}$, which correspond to the singlet neutron-proton scattering length and the saturation density of symmetric nuclear matter.

with $C_0(R_c)$ the coupling constant. Provided the wave function is known, the coupling and its running are given by

$$C_0(R_c) = \lim_{\epsilon \rightarrow 0^+} \frac{2\pi^2}{\mu} \left(\frac{u'_0(R_c + \epsilon)}{u_0(R_c + \epsilon)} - \frac{u'_0(R_c - \epsilon)}{u_0(R_c - \epsilon)} \right), \quad (23)$$

where $u_0(r) = r \Psi_0(r)$ is the zero-energy reduced two-body wave function.

But first one needs the two-body wave functions for a delta-shell potential. They can be obtained by solving the r-space Lippmann-Schwinger equation and its in-medium counterpart, leading to

$$\Psi_0(r) = 1 + \lambda G_0(r; R_c), \quad (24)$$

$$\Psi_{0,0}(r) = 1 + \mu K_0(r; R_c), \quad (25)$$

with λ, μ the same parameters that already appeared in Eqs. (11) and (12), and where the regularized two-body

propagators are given by

$$\begin{aligned} G_0(r; R_c) &= \int_0^\infty dx \delta(x - R_c) \int \frac{d^2 \hat{x}}{4\pi} G_0(|\vec{r} - \vec{x}|) \\ &= -\frac{m_N}{4\pi} \left[\frac{\theta(r - R_c)}{r} + \frac{\theta(R_c - r)}{R_c} \right], \end{aligned} \quad (26)$$

$$\begin{aligned} K_0(r; R_c) &= \int_0^\infty dx \delta(x - R_c) \int \frac{d^2 \hat{x}}{4\pi} K_0(|\vec{r} - \vec{x}|) \\ &= -\frac{m_N}{4\pi} \left[\frac{\theta(r - R_c)}{r} + \frac{\theta(R_c - r)}{R_c} \right. \\ &\quad \left. - \frac{2}{\pi r} \frac{f(k_F(r + R_c)) - f(k_F(r - R_c))}{2k_F R_c} \right], \end{aligned} \quad (27)$$

where the function f is defined as

$$f(x) = -1 + \cos x + x \text{Si}(x). \quad (28)$$

Thus when a cutoff is introduced the vacuum zero energy wave function changes to

$$\Psi_0(r) = 1 - a_0 \left[\frac{\theta(r - R_c)}{r} + \frac{\theta(R_c - r)}{R_c} \right], \quad (29)$$

in which it can be appreciated that the effect of the delta-shell is local: for $r < R_c$ one ends up with a free wave function, while only for $r > R_c$ are the effects of the regularized contact-range interaction felt. The corresponding in-medium wave function now changes to

$$\begin{aligned} \Psi_{0,0}(r) &= 1 - \frac{1}{\frac{1}{a_0} - \frac{2}{\pi} k_F} \left[\frac{\theta(r - R_c)}{r} + \frac{\theta(R_c - r)}{R_c} \right. \\ &\quad \left. - \frac{2}{\pi r} \frac{f(k_F(r + R_c)) - f(k_F(r - R_c))}{2k_F R_c} \right], \end{aligned} \quad (30)$$

where the second, k_F -dependent term in the parentheses is non-local. That is, the effects of the delta-shell are now felt for all r .

With the previous wave functions, one ends up with the couplings

$$\frac{1}{C_0(R_c)} = \frac{m_N}{4\pi} \left(\frac{1}{a_0} - \frac{1}{R_c} \right), \quad (31)$$

$$\frac{1}{C_{0F}(R_c)} = \frac{m_N}{4\pi} \left(\frac{1}{a_0} - \frac{2}{\pi} k_F - \frac{g_0(k_F R_c)}{R_c} \right), \quad (32)$$

for the vacuum and in-medium case, respectively, where

$$g_0(x) = 1 - \frac{1}{\pi} \frac{1}{x} (-1 + \cos(2x) + 2x \text{Si}(2x)). \quad (33)$$

Their runnings are computed in Fig. 2 for the specific case of $a_0 = -23.7 \text{ fm}$ and $k_F = 1.33 \text{ fm}^{-1}$, corresponding to singlet neutron-proton scattering and the saturation density of symmetric nuclear matter. As can be readily

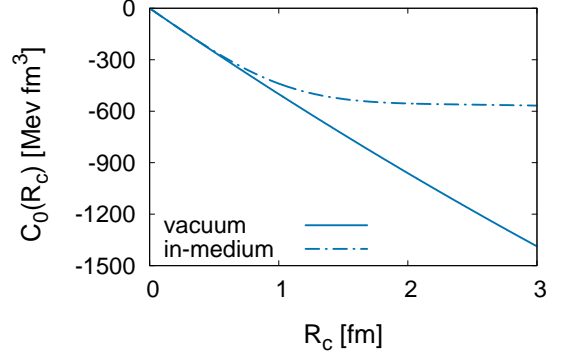


FIG. 2. Running of the lowest order coupling constant C_0 with respect to the r -space cutoff R_c in vacuum and in medium. The scattering length and Fermi momentum are the same as in Fig. 1.

noticed, the in-medium coupling RG evolution *freezes* at distances $R_c \geq (1 - 2) \text{ fm}$, in agreement with the naive intuition about its expected behavior.

It is also interesting to notice that the running of the in-medium coupling implicitly contains resummations of $a_0 k_F$, which could be considered a non-perturbative effect. Yet, here perturbativeness will be used in the sense of expanding in terms of powers of the couplings, regardless of whether the couplings contain resummations.

C. Infrared RG flow and power counting

The power counting of the lowest-order contact-range theory is easy to understand by evolving the couplings towards the infrared, defined as $Q R_c \rightarrow 1$ (i.e. $R_c \rightarrow \infty$ for $Q \rightarrow 0$), and then considering iterations of the contact within this limit.

For the delta-shell regulator the $R_c \rightarrow \infty$ limit of the running of the vacuum coupling is

$$\frac{1}{C_0(R_c \rightarrow \infty)} \rightarrow \frac{m_N}{4\pi} \frac{1}{a_0}. \quad (34)$$

Thus, depending on the size of the scattering length, this leads to the well-known scalings [39, 40]

$$C_0(R_c \sim 1/Q) \propto \frac{4\pi}{m_N} \frac{1}{M} \quad \text{for } a_0 \sim 1/M, \quad (35)$$

$$C_0(R_c \sim 1/Q) \propto \frac{4\pi}{m_N} \frac{1}{Q} \quad \text{for } a_0 \sim 1/Q. \quad (36)$$

For the in-medium coupling one has instead

$$\frac{1}{C_{0F}(R_c \rightarrow 0)} \rightarrow \frac{m_N}{4\pi} \left(\frac{1}{a_0} - \frac{2}{\pi} k_F \right), \quad (37)$$

yielding the infrared scalings

$$C_{0F}(R_c \sim 1/Q) \propto \frac{4\pi}{m_N} \frac{1}{M} \quad \text{for } \frac{2}{\pi} k_F a_0 \ll 1, \quad (38)$$

$$C_{0F}(R_c \sim 1/Q) \propto \frac{4\pi}{m_N} \frac{1}{Q} \quad \text{for } \frac{2}{\pi} k_F a_0 \gg 1, \quad (39)$$

which are like the vacuum ones but modified by the presence of the Fermi momentum.

If one now considers the iterations of the contact-range potential, their sizes are easily determined from the perturbative expansion of the Lippmann-Schwinger (Bethe-Goldstone) equation for the T- (G-) matrix. In the vacuum the expansion of the T-matrix is given by

$$\begin{aligned} T &= \sum_{n \geq 1} T_n = C_0(R_c) + G_0(R_c; R_c) C_0^2(R_c) + \dots \\ &= C_0(R_c) - \frac{m_N}{4\pi} C_0^2(R_c) \frac{1}{R_c} + \dots, \end{aligned} \quad (40)$$

where the subindex in T_n refers to the number of iterations of the contact-range coupling. From this, in the infrared limit the iterations scale as

$$\begin{aligned} -\frac{T_{n+1}}{T_n} &= \frac{m_N}{4\pi} C_0(R_c) \frac{1}{R_c} \\ &\rightarrow \frac{a_0}{R_c} \propto Q a_0, \end{aligned} \quad (41)$$

where the second line corresponds to the $R_c \rightarrow \infty$ limit. This implies a perturbative (non-perturbative) EFT if low-energy scattering is weak (strong).

If one now considers the in-medium case, the expansion of the G-matrix is given by

$$\begin{aligned} G &= \sum_{n \geq 1} G_n = C_{0F}(R_c) + K_0(R_c; R_c) C_{0F}^2(R_c) + \dots \\ &= C_{0F}(R_c) - \frac{m_N}{4\pi} C_{0F}^2(R_c) \frac{g_0(k_F R_c)}{R_c} + \dots, \end{aligned} \quad (42)$$

and thus in the infrared limit one has

$$\begin{aligned} -\frac{G_{n+1}}{G_n} &= \frac{m_N}{4\pi} C_{0F}(R_c) \frac{g_0(k_F R_c)}{R_c} \\ &\rightarrow +\frac{1}{2} \frac{\frac{2}{\pi} k_F}{\frac{1}{a_0} - \frac{2}{\pi} k_F} \frac{1}{(k_F R_c)^2}, \end{aligned} \quad (43)$$

which implies that loops are to be counted as

$$\frac{G_{n+1}}{G_n} \propto \frac{Q}{M} \frac{Q}{k_F} \quad \text{or} \quad \left(\frac{Q}{k_F} \right)^2 \quad (44)$$

for $a_0 \sim 1/M$ and $a_0 \sim 1/Q$, respectively.

This argument suggests that in nuclear matter (where the scattering length is large) the lowest order contact is to be iterated at all orders, which relates to previous discussions in the literature [41–43]. Yet, the infrared running of the loops is clearly different than in the vacuum, leaving room for their numerical suppression for

values of $k_F R_c$ still of order unity but somewhat larger than one.

If anything this asks for a more detailed examination of the behavior of the loops, particularly owing to the fact that the previous argument relies on their bare (i.e. cutoff dependent) evaluation. Thus, it can be improved by considering the renormalized loops instead, for which one includes corrections to the coupling constant that remove the cutoff dependence of the loops. For this, one expands the coupling around the infrared limit, which for the vacuum case yields

$$\begin{aligned} C_0(R_c) &= \frac{4\pi}{m_N} a_0 + \frac{4\pi}{m_N} \frac{a_0^2}{R_c} + \dots \\ &= C_0 + \delta C_0 + \dots, \end{aligned} \quad (45)$$

where in the present context C_0 refers to the finite part of $C_0(R_c)$ in the $R_c \rightarrow \infty$ limit and δC_0 to its first, cutoff-dependent correction. Now the perturbative series for the T-matrix reads

$$\sum_{n=0}^{\infty} T_n = C_0 + \delta C_0 - \frac{m_N}{4\pi} \frac{C_0^2}{R_c} + \dots \quad (46)$$

which leads to the conclusion that there are no perturbative corrections to the T-matrix at zero energy ($E = 0$), or equivalently, at zero on-shell momentum ($p = \sqrt{m_N E} = 0$):

$$T(p=0) = \frac{4\pi}{m_N} a_0 = C_0. \quad (47)$$

In hindsight this is trivial: at zero energy one can always rearrange the higher order corrections to the coupling in such a way that the T-matrix does not change.

Instead, what one has to consider is the expansion in terms of powers of the external momentum p , whose effect is to change the propagator to

$$G_0(R_c; R_c) = -\frac{m_N}{4\pi} \left[\frac{1}{R_c} + i p + \mathcal{O}(p^2) \right], \quad (48)$$

in which case one ends up with

$$\begin{aligned} T(p) &= C_0 + \delta C_0 - \frac{m_N}{4\pi} C_0^2 \left[\frac{1}{R_c} + i p \right] + \dots \\ &= \frac{4\pi}{m_N} a_0 (1 - i a_0 p + \dots), \end{aligned} \quad (49)$$

which recovers the first non-trivial term in the expansion of the T-matrix for a zero-range interaction, that is:

$$T(p) = \frac{4\pi}{m_N} \frac{1}{\frac{1}{a_0} + i p} = \frac{4\pi}{m_N} a_0 \sum_{n=0}^{\infty} (-i a_0 p)^n. \quad (50)$$

In turn, this also implies the well-known result that loops scale as $Q a_0$.

For the iteration of the in-medium coupling, one begins with the infrared expansion of the coupling itself

$$\begin{aligned} C_{0F}(R_c) &= \frac{4\pi}{m_N} \frac{1}{\frac{1}{a_0} - \frac{2}{\pi} k_F} \\ &+ \frac{4\pi}{m_N} \frac{1}{\left(\frac{1}{a_0} - \frac{2}{\pi} k_F\right)^2} \frac{g_0(k_F R_c)}{R_c} + \dots \\ &= C_{0F} + \delta C_{0F} + \dots, \end{aligned} \quad (51)$$

and then considers the expansion of the loops in powers of the external total and relative momenta

$$\begin{aligned} K_0(R_c; R_c) &= -\frac{m_N}{4\pi} \left[\frac{g_0(k_F R_c)}{R_c} \right. \\ &\left. + P g_1(k_F R_c) + \mathcal{O}(p^2, P^2) \right], \end{aligned} \quad (52)$$

where the term proportional to p vanishes (as scattering is suppressed below the Fermi sea). Here g_1 is given by

$$g_1(x) = -\frac{1}{\pi} \frac{1 - \cos(2x)}{(2x)^2}. \quad (53)$$

Thus, up to corrections proportional to P , the expansion of the G-matrix reads

$$\begin{aligned} G(q, Q) &= G + \delta G + \dots \\ &= C_0 + \delta C_0 \\ &- \frac{m_N}{4\pi} C_0^2 \left[\frac{g_0(k_F R_c)}{R_c} + P g_1(k_F R_c) + \dots \right] \\ &+ \dots, \end{aligned} \quad (54)$$

and, after removing the divergence at $p = P = 0$, the relative size of the corrections is

$$\begin{aligned} -\frac{\delta G}{G} &= \frac{1}{\frac{1}{a_0} - \frac{2}{\pi} k_F} \frac{P}{\pi} \frac{1 - \cos(2k_F R_c)}{(2k_F R_c)^2} \\ &\propto \left(\frac{Q}{k_F} \right) \frac{\sin^2(k_F R_c)}{2(k_F R_c)^2}, \end{aligned} \quad (55)$$

where the second line assumes $\frac{2}{\pi} a_0 k_F \gg 1$ (e.g. unnatural scattering length and nuclear matter equilibrium density).

This reproduces the previous estimate about the infrared scaling of the loops, but adds a new twist: the loop contributions might very well vanish at certain cut-offs. For the case at hand, the first r-space cutoff at which this particular loop contribution vanishes is $k_F R_c = \pi$.

In general, if one expands the in-medium loop function further in powers of P and p , then the individual terms in this expansion do not necessarily vanish at the same cut-offs (and some of them do not vanish at any cutoff). The proper comparison to be made is not the perturbative expansion of the G-matrix, but rather the perturbative expansion of the potential energy per nucleon (or per fermion).

This is nicely illustrated by considering the next two terms in the expansion of the propagator as a function of the external momenta, i.e. the terms proportional to p^2 and P^2 :

$$\begin{aligned} K_0(R_c; R_c) &= -\frac{m_N}{4\pi} \left[\frac{g_0(k_F R_c)}{R_c} + P g_{01}(k_F R_c) \right. \\ &+ \frac{p^2}{k_F} g_{2A}(k_F R_c) + \frac{P^2}{k_F} g_{2B}(k_F R_c) \\ &\left. + \mathcal{O}(p^3, P^3, Pp^2, P^2p) \right], \end{aligned} \quad (56)$$

with

$$\begin{aligned} g_{2A}(x) &= -\frac{2}{3} x + \frac{1}{3\pi x^2} + \frac{(2x^2 - 1) \cos(2x)}{3\pi x^2} \\ &+ \frac{\sin(2x)}{3\pi x} + \frac{4}{3\pi} x \text{Si}(2x), \end{aligned} \quad (57)$$

$$g_{2B}(x) = \frac{(2 \sin(x) - x \cos(x)) \sin x}{6\pi x^2}. \quad (58)$$

In this case the relative size of the renormalized loop corrections is

$$\begin{aligned} -\frac{\delta G}{G} &= \frac{m_N}{4\pi} C_0 \left[P g_1(k_F R_c) \right. \\ &+ \frac{p^2 g_{2A}(k_F R_c) + P^2 g_{2B}(k_F R_c)}{k_F} \\ &\left. + \mathcal{O}(p^3, P^3, pP^3) \right], \end{aligned} \quad (59)$$

where g_1 and g_{2B} do both have zeros, though not at the same cutoff, while g_{2A} is always positive. This indicates that power counting arguments solely grounded in the loop corrections to the G-matrix are not necessarily straightforward, as there is a certain cutoff asynchrony among the different terms in its low-momentum expansion. In contrast, if one considers the potential energy instead (as in [44, 45]), i.e., the average of the G-matrix in the medium, which is proportional to

$$\begin{aligned} (E + \delta E) &\propto \\ &\Omega \int_{k_1, k_2 < k_F} \frac{d^3 \vec{k}_1}{(2\pi)^3} \frac{d^3 \vec{k}_2}{(2\pi)^3} (G + \delta G), \end{aligned} \quad (60)$$

where Ω is the volume of the system, one arrives at

$$\begin{aligned} -\frac{\delta E}{E} &\propto \frac{m_N k_F}{4\pi} C_0 \left[\frac{36}{35} g_1(k_F R_c) \right. \\ &\left. + \frac{3}{10} g_{2A}(k_F R_c) + \frac{6}{5} g_{2B}(k_F R_c) + \dots \right], \end{aligned} \quad (61)$$

where the sum of the terms within the brackets do now have zeros in the infrared limit. For the three terms included in the brackets, the first zero happens at $k_F R_c \approx$

0.8498 (compatible with $QR_c \sim 1$, i.e., with the infrared limit).

If one were to include all the powers in the expansion on external momenta of $G(p, P)$ and $\delta G(p, P)$, one could simply write

$$\frac{\delta E}{E} \propto -\frac{m_N k_F}{4\pi} C_0 h_F(k_F R_c), \quad (62)$$

where the $h_F(x)$ function represents the relative strength of the loop contributions to the potential energy in nuclear matter. If scattering is strong at low energies, as is the case in the two-nucleon system, the expression simplifies to

$$\frac{\delta E}{E} \propto \frac{\pi}{2} h_F(k_F R_c), \quad (63)$$

which further cements the interpretation of h_F as the effective expansion parameter for the loops.

For the delta-shell regulator there is no analytical expression for $h_F(x)$, which has to be evaluated numerically instead. This is done in Fig. 3, where it can be appreciated that regardless of the cutoff the loops are numerically suppressed. The first zero of the function $h_F(x)$ happens at $x \approx 1.137$, followed by $x \approx 1.701$, then $x \approx 3.451$ and so on, which for $k_F = 1.33 \text{ fm}^{-1}$ (the equilibrium density of nuclear matter) translates into $R_c = 0.85, 1.28, 2.59 \text{ fm}$. Regardless of whether the loop contribution vanishes for a given cutoff, the fact is that $h_F(x)$ becomes rather small once the infrared regime ($x \geq 1$) is reached. This reinforces the observation that the loops are indeed suppressed in the infrared, hence implying a perturbative power counting for nuclear matter.

For assessing the regulator dependence of the previous result one might consider a sharp cutoff regulator in momentum space, for which the running of the in-medium coupling is

$$C_{0F}(\Lambda) = C_0(\Lambda) \theta(\Lambda - k_F) + C_0(k_F) \theta(k_F - \Lambda), \quad (64)$$

with $C_0(\Lambda)$ the vacuum running

$$\frac{1}{C_0(\Lambda)} = \frac{m_N}{4\pi} \left(\frac{1}{a_0} - \frac{2}{\pi} \Lambda \right). \quad (65)$$

That is, for a sharp cutoff the C_0 coupling *exactly* freezes for $\Lambda < k_F$, providing the ideal illustration of this phenomenon. The calculation of $h_F(x)$ can be done analytically in this case, though the expression is rather cumbersome (it can be found in Eq. (A50) of Appendix A for $x \leq 1/2$). Its numerical evaluation is shown in Fig. 3, where there are now only two zeros located at $x \approx 0.5592$ and $x \approx 0.9210$, with $x = k_F/\Lambda$. Even though the specific details of the infrared behavior are different from those of the delta-shell (for instance, the derivative of $h_F(x)$ shows a discontinuity at $x = 1$ corresponding to the one in the running of the in-medium coupling), the loops are nonetheless still suppressed.

It is also worth noticing that even in the ultraviolet limit ($x \rightarrow 0$) one finds that

$$h_F(0) = \frac{2}{\pi} - \frac{6(11 - 2 \log 2)}{35\pi} \approx 0.11203, \quad (66)$$

which is numerically small and regulator independent, where the second term is very familiar as it appears frequently in calculations of many-fermion systems (e.g. in [46] from the fifties). This limit is not entirely a curiosity in the sense that this also corresponds to the calculation of $h_F(x)$ in power divergence subtraction (PDS) [47, 48], a modification of dimensional regularization that is particularly well suited for the two-nucleon system¹.

In terms of power counting the conclusion is that in-medium loops are suppressed in the infrared limit with respect to their behavior in the vacuum. This suppression is not the usual one involving the Q/M ratio of the characteristic soft and hard scales of the theory, but a numerical one instead. Of course a warning is in place: this conclusion is dependent on relying on the in-medium running of the coupling and also on the choice of regulator, on which the numerical suppression depends. Indeed the arguments presented here require the use of the in-medium running. This often assumes full knowledge of the in-medium two-body wave function, which in general is not the case, precluding the exact calculation of the infrared limit of the in-medium running of the coupling. Of course there will be exceptions and certain regulators might provide remarkable simplifications.

With this limitation in mind, one might consider using the infrared limit of the vacuum coupling instead, Eq. (34). By repeating the previous arguments, one finds:

$$\frac{\delta E}{E} \propto a_0 k_F \left[h_F(k_F R_c) - \frac{2}{\pi} \right], \quad (67)$$

which results in the subtraction of a factor of $2/\pi$ to the dimensionless loop function $h_F(x)$. This factor originates from the difference between the infrared limits of $C_0(R_c)$ and $C_{0F}(R_c)$ and its interpretation is straightforward: the loop corrections are now forced to recover this difference, which is not perturbative (in the sense that C_{0F} contains resummations of $k_F a_0$ in the infrared).

Yet, there is a simple workaround grounded in a trivial observation: the value of the vacuum coupling at a finite

¹ A quirk of PDS is that the running of the vacuum and in-medium couplings is identical: for a contact-range theory, PDS is only able to see the linear divergence of the loop integrals at the expense of other types of cutoff dependence. That is, the healing distance sits squarely within the blind spot of PDS. Yet, there is a simple trick for being able to recycle the previous formalism with PDS, which is to reorder the coupling as

$$C_{0F}^{\text{PDS}}(\Lambda) = \frac{4\pi}{m_N} \frac{1}{\frac{1}{a_0} - \frac{2}{\pi} k_F - (\Lambda - \frac{2}{\pi} k_F)},$$

and expand in powers of $(\Lambda - \frac{2}{\pi} k_F)$.

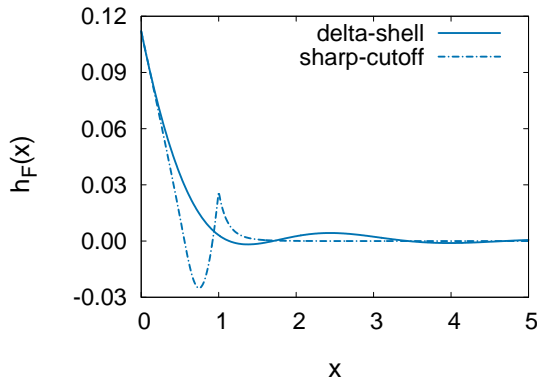


FIG. 3. The function $h_F(x)$, which determines the relative size of the loops in nuclear matter, as calculated for a delta-shell regulator in r-space and a sharp-cutoff in p-space. Here $x = k_F R_c$ or $x = k_F/\Lambda$ for the delta-shell and sharp-cutoff, respectively, with R_c and Λ the r-space and p-space cutoffs.

cutoff R_c^* is basically equivalent to the infrared limit of the in-medium coupling at some Fermi momentum k_F^* . For a contact-range theory and a delta-shell regulator the equivalence in the $R_c^* \rightarrow \infty$ limit is given by $k_F^* R_c^* = \pi/2$. Outside this limit, one might recalculate the renormalized loop correction

$$\frac{\delta E}{E} \propto -\frac{m_N}{4\pi} C_0(R_c^*) \left[\frac{1}{R_c^*} + k_F \left(h_F(k_F R_c) - \frac{2}{\pi} \right) \right], \quad (68)$$

then define the function

$$\bar{h}_F(x) = h_F(x) - \frac{2}{\pi}, \quad (69)$$

and from it, the equivalent Fermi momentum

$$1 + (k_F^* R_c^*) \bar{h}_F(k_F^* R_c^*) = 0, \quad (70)$$

leading to

$$\frac{\delta E}{E} \propto \frac{k_F^* \bar{h}_F(k_F^* R_c^*) - k_F \bar{h}_F(k_F R_c)}{k_F^* \bar{h}_F(k_F^* R_c^*)}. \quad (71)$$

This expression is not transparent until one considers the infrared limit, for which $\bar{h}_F \rightarrow -2/\pi$ (i.e. $h_F \rightarrow 0$), in which case:

$$\frac{\delta E}{E} \propto \frac{k_F^* - k_F}{k_F^*}. \quad (72)$$

That is, even if one does not know the exact running of the in-medium coupling (which explicitly depends on the Fermi momentum), it is still possible to use the vacuum coupling instead and choose a cutoff R_c^* such that loop corrections cancel for a Fermi momentum k_F^* , which depends on the previous cutoff. This will be the approach followed in the next Section.

III. POWER COUNTING IN NUCLEAR MATTER

Now I will consider nuclear matter, understood as a non-relativistic system of fermions with two (spin) or four (spin and isospin) degrees of freedom, where the first case corresponds to neutron matter and the second to symmetric nuclear matter. For simplicity, Wigner SU(4) will be assumed and only S-wave contact-range interactions will be examined in detail. The focus is on power counting, for which S-wave interactions probably provide the best example of how it works, and where the differences between singlet and triplet S-wave scattering are in principle not crucial. P-wave and higher orbital angular momentum interactions usually enter at subleading orders, and their power counting relies on the same set of ideas as S-wave interactions.

First, I will deal with the power counting of two-body forces, which illustrate the most important issues regarding the organization of EFT in nuclear matter. After that, I will briefly discuss three- and four-body forces.

A. The two-body potential

The form of the two-body contact-range potential depends on the explicit representation chosen for it. If one considers momentum-dependent interactions, it will be given by

$$V_{2B} = \sum_{n \geq 0} C_{2n}(\Lambda) \frac{1}{2} (p^{2n} + p'^{2n}), \quad (73)$$

with C_{2n} denoting the couplings and p, p' the initial and final relative momenta of the nucleons. Alternatively, one may use the energy-dependent representation

$$V_{2B} = \sum_{n \geq 0} C_{2n}(\Lambda) k^{2n}, \quad (74)$$

where $k = \sqrt{m_N E}$ with m_N the nucleon mass and E the center-of-mass energy of the two nucleons. It happens that in nuclear matter it is possible to switch energy-dependence with density-dependence, which leads to the following representation

$$V_{2B} = \sum_{n \geq 0} C_{2n}(\Lambda) k_F^{2n}, \quad (75)$$

where k_F is now the Fermi momentum. This last representation is the most convenient by far for dealing with nuclear matter, and is the one I will use as the default case.

The previous three representations are equivalent at tree level in terms of the equation of state (EOS). But the EOS is not an observable and this equivalence breaks down once loop corrections are included. Besides, while the momentum- and energy-dependent representation provide a direct bridge with two-nucleon forces and the

properties of two-nucleon systems (e.g. phase shifts and deuteron observables), this is not the case for the density-dependent representation, which can instead be thought as nuclear matter specific (here one may check [49] for an EFT-specific discussion of off-shell effects at finite density). It is also worth mentioning that density-dependent interactions induce thermodynamic instabilities in the EOS, which can nonetheless be corrected by the inclusion of additional terms [50].

B. Equation of state at tree level

At tree level, with the previous contact-range potential, one can easily calculate the energy per nucleon as

$$\begin{aligned} \frac{E}{A} &= \frac{\Omega}{A} \sum_{s_1} \int_{k_1 < k_F} \frac{d^3 \vec{k}_1}{(2\pi)^3} \frac{k_1^2}{2m} \\ &+ \frac{\Omega}{2A} \sum_{s_1, s_2} \int_{k_1, k_2 < k_F} \frac{d^3 \vec{k}_1}{(2\pi)^3} \frac{d^3 \vec{k}_2}{(2\pi)^3} \langle V_{2B} \rangle, \end{aligned} \quad (76)$$

where s_1, s_2 are the spins of nucleons 1, 2, and $\langle V_{2B} \rangle$ is the matrix element of V_{2B} when sandwiched between antisymmetric $|\vec{k}_1 s_1 \vec{k}_2 s_2\rangle_A$ two-body states.

If there are only S-wave two-body forces one arrives at the EOS

$$\frac{E}{A} = t \rho^{2/3} + c_0 \rho + c_2 \rho^{5/3} + \sum_{n \geq 2} c_{2n} \rho^{1+2n/3}, \quad (77)$$

where ρ is the density and t, c_{2n} parameters for the kinetic and potential energy terms. The density is given by

$$\rho = \sum_{s_1} \int_{k_1 < k_F} d^3 \vec{k}_1 = g \frac{k_F^3}{6\pi^2}, \quad (78)$$

with g the number of different spin states ($g = 2$ for neutron matter and 4 for symmetric nuclear matter). Meanwhile, t is given by

$$t = \frac{3}{5} \left(\frac{6\pi^2}{g} \right)^{2/3} \frac{1}{2m_N}, \quad (79)$$

while the c_{2n} coefficients read (in the density-dependent representation) as

$$c_{2n} = \frac{1}{2} \left(1 - \frac{1}{g} \right) C_{2n}(\Lambda) \left(\frac{6\pi^2}{g} \right)^{2n/3}. \quad (80)$$

C. Loops and the divergence structure

The one-loop correction to the tree level EOS can be written as

$$\frac{\delta E}{A} = \frac{\Omega}{4A} \sum_{s_1, s_2} \int_{k_1, k_2 < k_F} \frac{d^3 \vec{k}_1}{(2\pi)^3} \frac{d^3 \vec{k}_2}{(2\pi)^3} \langle V_{2B} \frac{Q_F}{e_{12}} V_{2B} \rangle, \quad (81)$$

where the matrix element corresponding to the first iteration of the two-body potential is given by

$$\langle V_{2B} \frac{Q_F}{e_{12}} V_{2B} \rangle = \int \frac{d^3 \vec{p}'}{(2\pi)^3} \frac{|\langle \vec{p} | V_{2B} | \vec{p}' \rangle|^2}{e_{12}} Q_F, \quad (82)$$

with e_{12} being the energy denominator

$$\begin{aligned} e_{12} &= \frac{k_1^2}{2m_N} + \frac{k_2^2}{2m_N} - \frac{k_1'^2}{2m_N} - \frac{k_2'^2}{2m_N} \\ &= \frac{p^2}{m_N} - \frac{p'^2}{m_N}, \end{aligned} \quad (83)$$

which only depends on the initial and final relative momenta \vec{p} and \vec{p}' (as the total momentum is conserved in the loops), and with Q_F a projector into states over the Fermi momentum

$$Q_F = \theta(k_1' - k_F) \theta(k_2' - k_F), \quad (84)$$

where

$$\begin{aligned} \vec{k}_1 &= \frac{\vec{P}}{2} + \vec{p} & \vec{k}_2 &= \frac{\vec{P}}{2} - \vec{p}, \\ \vec{k}_1' &= \frac{\vec{P}'}{2} + \vec{p}' & \vec{k}_2' &= \frac{\vec{P}'}{2} - \vec{p}'. \end{aligned} \quad (85)$$

That is, I am using \vec{k}_j, \vec{k}_j' for the momentum of the individual particles, and \vec{P}, \vec{p} and \vec{P}', \vec{p}' for the total and center-of-mass momenta. Owing to momentum conservation in the loops, one has that $\vec{P} = \vec{P}'$.

The loop integral is divergent and requires regularization. By simply cutting it at $p = \Lambda$ and focusing on the linear divergence, one obtains

$$\begin{aligned} \langle V \frac{Q_F}{e_{12}} V \rangle &= -\frac{m_N}{2\pi^2} \Lambda \\ &\times [C_0^2 + 2C_0 C_2 k_F^2 + (C_2^2 + 2C_0 C_4) k_F^4 + \dots] \\ &+ (\text{finite terms}), \end{aligned} \quad (86)$$

where it is now apparent why the density-dependent representation has been chosen. By integrating over the initial momenta (which are all below the Fermi momentum) and rearranging the terms one arrives at

$$\begin{aligned} \frac{E}{A} + \frac{\delta E}{A} &= t \rho^{2/3} \\ &+ [c_0 + \delta c_0 + \lambda_0 c_0^2 \Lambda] \rho \\ &+ [c_2 + \delta c_2 + 2\lambda_0 c_0 c_2 \Lambda] \rho^{5/3} \\ &+ [c_4 + \delta c_4 + \lambda_0 (c_2^2 + 2c_0 c_4) \Lambda] \rho^{7/3} \\ &+ \dots, \end{aligned} \quad (87)$$

where the dots indicate either finite terms or divergent terms involving higher powers of the density, while λ_0 is a numerical constant.

From this it is apparent that the iteration of C_0 does not generate new divergent terms depending on higher

powers of the density and is thus self-contained. In the spirit of the arguments given in [21, 22] this defines a natural candidate for the lowest-order approximation, one in which only C_0 is included, and for which the first loop correction is given by

$$\frac{E}{A} + \frac{\delta E}{A} = t\rho^{2/3} + c_0\rho + [\delta c_0 + \lambda_0 c_0^2 \Lambda] \rho + \dots, \quad (88)$$

where the dots indicate finite contributions only (which for C_0 have a density dependence of $\rho^{4/3}$). By decomposing the loop correction into a renormalized and divergent part

$$\delta c_0 = \delta c_0^R - \lambda_0 c_0^2 \Lambda, \quad (89)$$

one ends up with

$$\frac{E}{A} + \frac{\delta E}{A} = t\rho^{2/3} + (c_0 + \delta c_0^R)\rho + \dots, \quad (90)$$

which basically only induces a finite correction to the c_0 parameter. This correction could in principle be zero if the original c_0 parameter has been optimally chosen in the first place.

In contrast, the corrections to the C_2 , C_4 and higher derivative couplings are not self-contained and include divergent terms dependent on higher powers of the density (this point is intimately related to the discussion in [21–24], though there other types of density-dependent terms usually appearing in the Skyrme forces are considered). Yet, as in the previous case, they only induce finite corrections to the c_2 , c_4 , \dots , parameters, i.e.

$$\begin{aligned} \frac{E}{A} + \frac{\delta E}{A} &= t\rho^{2/3} + (c_0 + \delta c_0^R)\rho \\ &+ [c_2 + \delta c_2^R] \rho^{5/3} + [c_4 + \delta c_4^R] \rho^{7/3} \\ &+ \dots, \end{aligned} \quad (91)$$

which again indicates that by choosing the parameters carefully at the first order at which they appear, their loop corrections can become trivial.

D. Power counting

To determine the power counting, as a first approximation one might simply apply the counting rules of two-body scattering in the vacuum to nuclear matter. That is, one begins with a strongly interacting two-body system in which the lowest order contact and the range correction scale as

$$C_0 \sim Q^{-1} \quad \text{and} \quad C_2 \sim Q^{-2}, \quad (92)$$

which is the usual scaling in pionless [39, 40], KSW [47, 48] and pionful EFT [51–58] (though in this last case, only in the singlet). Next, one counts the loops as

$$\int \frac{d^3 \vec{q}'}{(2\pi)^3} m_N \frac{\theta(k'_1 - k_F) \theta(k'_2 - k_F)}{q^2 - q'^2} \sim Q, \quad (93)$$

and then deduces the counting of the higher order contacts from the condition of including the new contacts when they are needed to absorb the divergences. This leads to the following naive counting for the different contributions to the EOS:

$$\begin{aligned} \frac{E}{A} &= \underbrace{t\rho^{2/3} + c_0\rho}_{Q^2(\text{LO})} + \underbrace{c_2\rho^{5/3}}_{Q^3(\text{NLO})} + \underbrace{c_4\rho^{7/3}}_{Q^4(\text{N}^2\text{LO})} \\ &+ \sum_{n=3}^{\infty} \underbrace{c_{2n}\rho^{1+2n/3}}_{Q^{n+2}(\text{N}^n\text{LO})}, \end{aligned} \quad (94)$$

which is quite simple, though for C_{2n} with $n > 1$ it differs from the vacuum counting.

Indeed, one ends up with $C_4 \sim Q^{-3}$, $C_6 \sim Q^{-4}$, etc., instead of the usual $C_{2n} \sim Q^{-2}$ for $n \geq 1$. Yet, if one were to determine the vacuum power counting from the perturbative divergence arguments above, one would have also arrived to the $C_{2n} \sim Q^{-(n+1)}$ scaling. This suggests that it might be a limitation of the present argument (as will be discussed in a few paragraphs), which after all only considers the naive divergence structure. However, it is worth mentioning here that this enhancement of the C_{2n} couplings coincides with the one proposed by Long and Yang in pionful EFT on the basis of analyzing their size in dimensional regularization [58].

Irrespective of the scaling of the C_{2n} couplings, there is still a contradiction though with the previous, naive power counting for the loops: it implies that many-body perturbation theory must be resummed at all orders for C_0 , which is inconsistent with the LO form of the EOS proposed here. Indeed, if a loop counts as Q and C_0 counts as Q^{-1} , then the full resummation of C_0 becomes necessary.

To understand why this is not the case at finite density, one begins by considering the explicit expression for the second order perturbative correction to the EOS:

$$\begin{aligned} \frac{E + \delta E}{A} &= t\rho^{2/3} + \frac{1}{2}(1 - \frac{1}{g})\rho \left[(C_0 + \delta C_0) \right. \\ &\left. + \left(\frac{g}{\rho}\right)^2 I_{0F}(k_F, \Lambda) C_0^2 + \dots \right], \end{aligned} \quad (95)$$

where the loop integral (averaged for two-body states below the Fermi momentum) is given by

$$I_{0F}(k_F, \Lambda) = \int_{k_1, k_2 < k_F} \frac{d^3 \vec{k}_1}{(2\pi)^3} \frac{d^3 \vec{k}_2}{(2\pi)^3} \int_{\Lambda} \frac{d^3 \vec{q}'}{(2\pi)^3} \frac{Q_F}{e_{12}}, \quad (96)$$

with the Λ subscript indicating that the integral has been regularized. This integral is analytically calculable with PDS, for which its evaluation yields

$$\begin{aligned} I_{0F}^{\text{PDS}}(k_F, \Lambda) &= -\frac{1}{(2\pi^2)^2} \left[\frac{m_N}{36\pi} \Lambda k_F^6 \right. \\ &\left. - \frac{m_N}{210\pi^2} (11 - 2 \log 2) k_F^7 \right]. \end{aligned} \quad (97)$$

Then the EOS can be rewritten as

$$\frac{E + \delta E}{A} = t \rho^{2/3} + \frac{1}{2} \left(1 - \frac{1}{g}\right) \rho \times \left[C_0 + \delta C_0 - C_0^2 \frac{m_N}{4\pi} (\Lambda - c_{0F} k_F) + \dots \right], \quad (98)$$

with c_{0F} a number, which in PDS is given by

$$c_{0F} = \frac{6}{35\pi} (11 - 2 \log 2) \approx 0.5246. \quad (99)$$

It is worth noting that this number is also the ultraviolet limit of the loop suppression function $\bar{h}_F(x)$ defined in Eq. (69). That is, $\bar{h}_F(0) = c_{0F}$.

Now, if one considers the RG evolution of the vacuum coupling in pionless EFT with PDS (with a_0 the scattering length)

$$C_0(\Lambda) = \frac{4\pi}{m_N} \frac{1}{\frac{1}{a_0} - \Lambda}, \quad (100)$$

one may build the expansion for the EOS around the infrared limit ($\Lambda \rightarrow 0$) of the vacuum ($k_F \rightarrow 0$), in which case one can expand the running of the vacuum coupling as

$$\begin{aligned} C_0(\Lambda) &= \frac{4\pi}{m_N} a_0 + \frac{4\pi}{m_N} a_0 (a_0 \Lambda) + \dots \\ &= C_0(\Lambda = 0) + \delta C_0(\Lambda) + \dots \end{aligned} \quad (101)$$

By explicitly including this expansion in the loop correction (i.e., in the second line of Eq. 98), one finds that

$$\begin{aligned} C_0 + \delta C_0 - C_0^2 \frac{m_N}{4\pi} (\Lambda - c_{F0} k_F) + \dots \\ = \frac{4\pi}{m_N} a_0 (1 + c_{0F} a_0 k_F + \dots), \end{aligned} \quad (102)$$

which indicates that the loop is indeed counted as k_F (i.e. Q) and thus, if $a_0 \sim 1/Q$ (strong scattering) the loops must be resummed. This reproduces the power counting in the vacuum, which requires the iteration of the contact-range coupling. Conversely, if $a_0 \sim 1/M$ (weak scattering), it reproduces the counting for dilute Fermi systems [59] (as this counting only requires $k_F a_0 \ll 1$ to be valid).

In contrast, if one expands the running of $C_0(\Lambda)$ around the cutoff Λ^* :

$$\begin{aligned} \frac{1}{C_0(\Lambda)} &= \frac{m_N}{4\pi} \left(\frac{1}{a_0} - \Lambda \right) \\ &= \frac{m_N}{4\pi} \left(\frac{1}{a_0} - \Lambda^* + (\Lambda^* - \Lambda) \right) \\ &= \frac{1}{C_0(\Lambda^*)} + \frac{m_N}{4\pi} (\Lambda^* - \Lambda), \end{aligned} \quad (103)$$

then one obtains the renormalized correction

$$\begin{aligned} C_0 + \delta C_0 - C_0^2 \frac{m_N}{4\pi} (\Lambda - c_F k_F) + \dots \\ = C_0(\Lambda^*) - C_0^2(\Lambda^*) \frac{m_N}{4\pi} (\Lambda^* - c_{0F} k_F) + \dots, \end{aligned} \quad (104)$$

which implies that the actual size of loop contributions is $(\Lambda^* - c_{0F} k_F)$. Formally, this still means that the loop scales as Q . Yet, it is apparent that by rewriting

$$\Lambda^* = c_{0F} k_F^*, \quad (105)$$

then the loop corrections vanish for the approximate Fermi momentum at which the RG flow freezes for the in-medium running of the coupling:

$$\begin{aligned} C_0 + \delta C_0 - C_0^2 \frac{m_N}{4\pi} (\Lambda - c_F k_F) + \dots \\ C_0(\Lambda^*) - C_0^2(\Lambda^*) \frac{m_N}{4\pi} c_{0F} (k_F^* - k_F) + \dots, \end{aligned} \quad (106)$$

which in turn means that the correct counting of the loops is $(k_F^* - k_F)$, with k_F^* the Fermi momentum for which the effective contact-range potential has been optimized.

By choosing the cutoff Λ^* what one is doing is optimizing the EOS for $k_F^* = \Lambda^*/c_{0F}$ in PDS, while for other regulators the only difference is the exact value of the proportionality constant between Λ^* and k_F^* . For the Fermi momentum k_F^* (or its corresponding density ρ^*), the first loop correction coming from the loops vanishes, while for Fermi momenta close to this value the loop corrections will be suppressed by a $(k_F^* - k_F)$ factor. That is, the EFT expansion is configured in terms of two expansion parameters, the familiar Q and the new $(k_F^* - k_F)$.

The natural choice for k_F^* in symmetric nuclear matter is around the saturation point, i.e. $k_F^* \approx 266$ MeV, while for neutron matter other choices could be tried depending on which densities one is interested in. With this, the preferred cutoff in PDS is $\Lambda^* \approx 140$ MeV at saturation density, where the C_0 coupling constant is

$$\begin{aligned} C_0(\Lambda^*) &= \frac{4\pi}{m_N} \frac{1}{\frac{1}{a_0} - \Lambda^*} = -\frac{4\pi}{m_N \Lambda^*} \left(1 + \mathcal{O}\left(\frac{1}{a_0 \Lambda^*}\right) \right) \\ &\approx -1158 \text{ MeV fm}^3, \end{aligned} \quad (107)$$

whose value is very similar to the ones usually appearing for the analogous t_0 parameter in the Skyrme potentials.

It might be possible though to derive the strength of the Skyrme parameters without resort to the equilibrium density, but from the behavior of the (pionful) wave functions by defining a healing renormalization scale [60]. This suggests the existence of further RG avenues from which to derive the equilibrium density of nuclear matter (instead of using it as an input) that will be worth exploring in the future.

The extension to the subleading contact-range interactions is not entirely trivial in regards to power counting. If one begins with C_2 , whose running in pionless EFT with PDS is given by

$$C_2(\Lambda) = \frac{m_N}{4\pi} C_0^2(\Lambda) \frac{r_0}{2}, \quad (108)$$

expands around $\Lambda = \Lambda^*$

$$\begin{aligned} C_2(\Lambda) &= \frac{m_N}{4\pi} C_0^2(\Lambda^*) \frac{r_0}{2} \\ &+ \left(\frac{m_N}{4\pi}\right)^2 C_0^3(\Lambda^*) r_0 (\Lambda - \Lambda^*) \\ &+ \mathcal{O}\left((\Lambda - \Lambda^*)^2\right), \end{aligned} \quad (109)$$

and then renormalizes the loop correction perturbatively

$$\begin{aligned} C_2 + \delta C_2 - 2 C_0 C_2 \frac{m_N}{4\pi} (\Lambda - c_{2F} k_F) + \dots \\ = C_2(\Lambda^*) - 2 C_0(\Lambda^*) C_2(\Lambda^*) \frac{m_N}{4\pi} (\Lambda^* - c_{2F} k_F) \\ + \dots, \end{aligned} \quad (110)$$

then it is apparent that the power counting structure of the loops has not changed, except for a detail: the new numerical constant c_{2F} . Its value depends on the chosen representation for the contacts. For the momentum-, energy- and density-dependent representations one obtains, respectively:

$$c_{2F} = \frac{1336 - 192 \log 2}{378\pi} \approx 1.0130, \quad (111)$$

$$c_{2F} = \frac{632 - 192 \log 2}{378\pi} \approx 0.4201, \quad (112)$$

$$c_{2F} = \frac{6}{35\pi} (11 - 2 \log 2) \approx 0.5246, \quad (113)$$

where for the density-dependent case the factor is identical to the one when C_0 is iterated (i.e. to c_{0F}).

This means that in general the Fermi momentum at which the first loop correction is perfectly suppressed depends on the order of the coupling (and on the regulator choice and representation of the contact-range interaction, which is perfectly acceptable as one is not dealing with an observable). However, this is not a problem in the sense that the iteration of these couplings is already suppressed in the first place owing to their scaling.

Another coupling that deserves a detailed analysis is C_4 , which in pionless EFT contains two contributions with different scalings

$$\begin{aligned} C_4(\Lambda) &= \frac{C_2^2(\Lambda)}{C_0(\Lambda)} + \frac{m_N}{4\pi} C_0^2(\Lambda) v_2, \\ &= C_4^A(\Lambda) + C_4^B(\Lambda), \end{aligned} \quad (114)$$

where C_4^A absorbs the cutoff dependence from the iteration of C_2 , while C_4^B contains the physical information about the shape parameter v_2 . As is well known, in the vacuum C_4^A enters at N²LO and C_4^B at N³LO. Owing to the linear nature of the contributions, it is possible to analyze their loop corrections separately. For C_4^A , by repeating the same steps as for C_2 , one has

$$\begin{aligned} C_4^A + \delta C_4^A - [C_2^2 + 2 C_0 C_4^A] \frac{m_N}{4\pi} (\Lambda - c_{4F}^A k_F) + \dots \\ = C_4^A(\Lambda^*) - \left[C_2^2(\Lambda^*) \right. \\ \left. + 2 C_0(\Lambda^*) C_4^A(\Lambda^*) \right] \frac{m_N}{4\pi} (\Lambda^* - c_{4F}^A k_F) \\ + \dots, \end{aligned} \quad (115)$$

while for C_4^B

$$\begin{aligned} C_4^B + \delta C_4^B - 2 C_0 C_4^B \frac{m_N}{4\pi} (\Lambda - c_{4F}^B k_F) + \dots \\ = C_4^B(\Lambda^*) - 2 C_0(\Lambda^*) C_4^B(\Lambda^*) \frac{3 m_N}{8\pi} (\Lambda^* - c_{4F}^B k_F) \\ + \dots, \end{aligned} \quad (116)$$

with c_{4F}^A and c_{4F}^B new numerical constants. In the momentum-dependent representation of the couplings their values are

$$c_{4F}^A = \frac{5636 - 564 \log 2}{891\pi} \approx 1.874, \quad (117)$$

$$c_{4F}^B = \frac{2}{3} \frac{6329 - 564 \log 2}{891\pi} \approx 1.414, \quad (118)$$

in the energy-dependent representation one has

$$c_{4F}^A = \frac{1337 - 564 \log 2}{891\pi} \approx 0.3380, \quad (119)$$

$$c_{4F}^B = \frac{2}{3} c_{4F}^A \approx 0.2253, \quad (120)$$

and finally, in the density-dependent representation they take their most simple form:

$$c_{4F}^A = c_{0F} \quad \text{and} \quad c_{4F}^B = \frac{2}{3} c_{0F}. \quad (121)$$

It is thus evident that the cutoff asynchrony of the iteration of higher derivative couplings increases with the order, where now this effect happens even for the density-dependent couplings (when dealing with the part of said couplings that contains new physical information).

Independently of the representation, the present analysis indicates that, in principle, the two contributions to C_4 are counted differently not only in the vacuum, but in nuclear matter as well. That is, the scalings still are

$$C_4^A \sim \frac{1}{Q^3} \quad \text{and} \quad C_4^B \sim \frac{1}{Q^2}. \quad (122)$$

It is necessary to emphasize *in principle* because this counting is only possible provided one includes counterterms of the C_4^A type in the first place. That is, counterterms that do not carry physical information but are there to remove the residual cutoff dependence. This type of counterterm has been explicitly identified in [61–63], where they have been called redundant or auxiliary.

To summarize, the features of the power counting of two-body contact-range forces in nuclear matter are:

- (i) The couplings scale *a priori* in exactly the same way as in the vacuum: the LO coupling is counted as $1/Q$. However, for subleading couplings this requires the inclusion of auxiliary couplings removing the residual cutoff dependence. Without them certain subleading couplings will require promotions.
- (ii) If the couplings are evaluated at the cutoff $\Lambda = \Lambda^*$, then their iteration in a loop counts as a factor of

$(k_F^* - k_F)$, with k_F^* a Fermi momentum proportional to Λ^* (where the proportionality constant also depends on the number of derivatives of the contact-range interaction)

- (iii) Formally this is compatible with how loops are counted in the vacuum (i.e., as Q), except for the fact that in the medium loops will be suppressed at Fermi momenta close to k_F^* .
- (iv) The practical consequence is that there is a Fermi momentum k_F^* in the vicinity of which the iterations of the LO coupling (evaluated at the cutoff Λ^*) are suppressed.
- (v) For subleading couplings this is also the case, though their k_F^* might be different than for the LO coupling. Nonetheless, this is inconsequential as their iterations are suppressed regardless of whether loops are counted as Q or $(k_F^* - k_F)$.

It is important to notice here that Λ^* is not really a cutoff, but the healing scale for nuclear matter with Fermi momentum k_F^* . By tuning the cutoff one is optimizing the EFT as to describe nuclear matter at a given density.

Yet, the $(k_F^* - k_F)$ counting rule is by itself the consequence of structuring nuclear matter calculations around the vacuum contact-range couplings (whose running does not depend on k_F) instead of the in-medium couplings (whose running depends on k_F), as already discussed at the end of Section II.

E. Derivative and primitive countings

Basically there are two possibilities regarding the power counting of subleading order terms, both of which renormalize the perturbative corrections to the energy per nucleon. One is a primitive or bottom-up approach, where new couplings are included wherever a divergence enters in this perturbative expansion. In pionless EFT this leads to the scaling $C_{2n} \sim 1/Q^{n+1}$.

Another is a derivative or top-down approach, where the starting point is the power counting of the couplings in the vacuum, and which explicitly requires the inclusion of auxiliary or redundant counterterms. In the vacuum this type of counterterm absorbs residual cutoff dependence, that is, cutoff dependence that vanishes in the hard cutoff limit. In the medium, if one expands around the MF limit (which corresponds to the infrared limit of the renormalization group), then this residual cutoff dependence is no longer residual and manifests as divergences. Thus, the inclusion of auxiliary counterterms turns out to be crucial if the original power counting of the two-nucleon system in the vacuum is to be kept.

This point might be illustrated with the specific example of the first iteration of the range correction to the

T-matrix in the vacuum:

$$\begin{aligned} \delta T &= \frac{1}{(1 - C_0 I_0)^3} [C_4^A + C_2^2 I_0] k^4 \\ &= \frac{4\pi}{m_N} \frac{1}{\left(\frac{1}{a_0} + ik\right)^3} \left[-\frac{m_N}{4\pi} C_4^A \left(\Lambda - \frac{1}{a_0}\right)^3 k^4 \right. \\ &\quad \left. + \left(\frac{1}{2} r_0 k^2\right)^2 \frac{\Lambda + ik}{\Lambda - \frac{1}{a_0}} \right], \end{aligned} \quad (123)$$

where the second line corresponds to its evaluation in PDS regularization with the runnings of C_0 and C_2 in pionless EFT. If one interprets the PDS renormalization scale Λ as a cutoff, or alternatively, if one treats the calculation in PDS as a simplified calculation in cutoff regularization, it is apparent that as $\Lambda \rightarrow \infty$ the contribution from the iteration of the range correction is finite and converges to the value it should be expected to have from the expansion of range corrections in the T-matrix:

$$\begin{aligned} T &= -\frac{4\pi}{m_N} \frac{1}{-\frac{1}{a_0} + \frac{1}{2} r_0 k^2 - ik} \\ &= +\frac{4\pi}{m_N} \frac{1}{\frac{1}{a_0} + ik} \sum_{n=0}^{\infty} \left(-\frac{\frac{1}{2} r_0 k^2}{\frac{1}{a_0} + ik} \right)^n. \end{aligned} \quad (124)$$

That is, C_4^A is unnecessary for the $\Lambda \rightarrow \infty$ limit to be well-defined. But if one were to expand all the loops, one would find instead

$$\begin{aligned} \delta T_{\text{exp}} &= [C_4^A + C_2^2 I_0] k^4 \sum_{n=0}^{\infty} (C_0 I_0)^n \\ &= \left[C_4^A - C_2^2 \frac{m_N}{4\pi} (\Lambda + ik) \right] k^4 \left(1 + \mathcal{O}(C_0 I_0) \right), \end{aligned} \quad (125)$$

where by considering the expansion of $C_2(\Lambda)$ around $\Lambda = 0$ it becomes evident that C_4^A now cures a divergence, a different role from the one it originally had in the calculation where the C_0 bubbles were resummed.

While this is but a curiosity in the two-body sector, in nuclear matter it becomes crucial, at least if one wants a microscopic derivation of the EOS (provided one is expanding around the MF approximation). The issue is that most two-body EFT descriptions ignore the existence of auxiliary counterterms, as they are not required to ensure renormalizability, understood usually as the existence of the ultraviolet limit. The only exception are improved actions [64–66], though they are currently limited to LO.

F. Pion exchanges

While there are clean arguments of why the loops of the contacts are suppressed at finite densities (or, at least, at

a given density), it is not evident if this is also the case for pion exchanges. There are reasons for their suppression too, though they belong to the category of educated guesses rather than that of concrete proof.

The question can be narrowed down to what happens with the pion loops in pionful EFT. In pionless there are no pion exchanges, while in KSW pion exchanges are counted as in naive dimensional analysis, that is:

$$V_F = \underbrace{V_{\text{OPE}}}_{Q^0} + \underbrace{V_{\text{TPE(L)}}}_{Q^2} + \underbrace{V_{\text{TPE(SL)}}}_{Q^3} + \dots, \quad (126)$$

where OPE refers to one-pion exchange, and TPE(L) and (SL) to leading and subleading two-pion exchange. Thus, pion contributions enter at NLO in the EOS.

If one now considers pionful EFT (or, more properly, the pionful EFT where OPE is non-perturbative), consistency requires that pion corrections to the running of the contact-range couplings follow their iteration pattern. That is, a coupling in pionful EFT receives a contribution from OPE at tree level, then a one-loop OPE contribution and a one-loop contribution from itself, and so on *ad infinitum*. Thus, if one wants the expansion of the couplings in nuclear matter to be consistent with the pion exchanges, the latter should in principle follow the iteration pattern of the former.

This issue is intertwined with the fact that what matters at finite density is the infrared running of the couplings for $\Lambda \rightarrow \Lambda^*$. With cutoffs Λ^* of the order of the pion mass at equilibrium density, it happens that pions are effectively perturbative at these regularization scales.

Besides, it is worth noticing that the running of the couplings in the presence of the OPE potential can be reproduced perturbatively until the appearance of the first deeply bound state generated by OPE. The reason is that perturbation theory for an attractive singular, power-law potential converges to the two-body wave function beyond its first zero (see [63] for a concrete example using the van der Waals potential). Owing to the fact that the couplings can be calculated from the form of the wave function, this means that the running of the coupling can be reproduced until the first zero of the wave function, at which point the non-perturbative coupling hits a singularity thus signaling the failure of perturbation theory.

Yet, for connecting the few-body description of nuclear forces with the properties of nuclear matter, it is enough to reproduce the running of the couplings in the vicinity of Λ^* , which does not require higher order perturbation theory. If high enough orders are involved though, matching the vacuum and the in-medium renormalizations will require the addition of auxiliary counterterms simply because the divergence structures are not identical for the perturbative and non-perturbative calculations.

But while perturbation theory for the OPE potential converges for the couplings, it does not for two-nucleon scattering. There perturbative pions fail at center-of-mass momenta of the order of (100 – 200) MeV, at which

the tensor part of the OPE potential requires a non-perturbative treatment [52, 67]. It is not clear though how this limitation manifests at finite density. For the EOS of nuclear matter the loop integrals are evaluated at external momenta below k_F while the internal momenta over which the loop runs are above k_F . This by itself does not imply that tensor OPE will be perturbative in nuclear matter, but is a strong hint in that direction.

G. Breakdown scale

There exists a clear analogy between scattering in the two-nucleon system and the perturbative expansion of the energy per nucleon in terms of the two-nucleon potential. They respectively involve the expansions of the T- and G-matrices, for which the only substantive difference is the inclusion of the projector Q_F in the second. In particular, they are completely analogous in what regards the distinction of long- and short-range physics. If one were to consider a generic two-body potential containing a long- and short-range component

$$V = V_L + V_S, \quad (127)$$

the two-potential formulas for the T- and G-matrices are formally equivalent

$$T = T_S + (1 + T_S \frac{1}{E - H_0}) \hat{T}_L (\frac{1}{E - H_0} T_S + 1), \quad (128)$$

$$G = G_S + (1 + G_S \frac{Q_F}{E - H_0}) \hat{G}_L (\frac{Q_F}{E - H_0} G_S + 1), \quad (129)$$

with T_S and \hat{T}_L defined as

$$\begin{aligned} T_S &= V_S + V_S \frac{1}{E - H_0} T_S, \\ \hat{T}_L &= V_L + V_L \frac{1}{E - H_0 - V_S} \hat{T}_L, \end{aligned} \quad (130)$$

and G_S and \hat{G}_L defined analogously, but with a Q_F projector over every energy denominator. The point is that the expansions of T and G in powers of m_L/m_S , or more generally light over heavy scales, will be really similar in both cases, with the main difference being that G contains k_F and the total momentum of the two fermions as new light scales. Notice that this idea has been previously discussed in [44] by means of a concrete calculation in a contact-range theory.

However, though the EOS depends on the G-matrix and its expansion, this does not imply that the analogy between the T- and G-matrix translates into similar expansion parameters for two-body scattering and the EOS. Here one has to explicitly check that the averaging over states within the Fermi sea does not alter the properties of the expansion.

A more transparent analogy between two-body scattering and the two-body potential energy per nucleon is provided by considering the perturbative effects of the short-range potential

$$V_S(\vec{q}) \propto \frac{g_S^2}{m_S^2 + \vec{q}^2}, \quad (131)$$

which corresponds to the exchange of a heavy meson of mass m_S . The perturbative effect on $\cot \delta(k)$ (with $\delta(k)$ the phase shift) is

$$\delta(\cot \delta) = m_N k \langle \Psi_k | V_S | \Psi_k \rangle, \quad (132)$$

with $|\Psi_k\rangle$ the two-body wave function in a normalization that asymptotically approaches the S-wave projection of $|\vec{k}\rangle$. Irrespective of the details of the wave function, one will find a contribution behaving as

$$\delta(\cot \delta(k)) \propto \log\left(1 + \frac{4k^2}{m_S^2}\right), \quad (133)$$

which implies the existence of a left branch cut starting a $k = \pm i(m_S/2)$ and hence that the Taylor expansion of $\cot \delta$ in powers of k only converges for $k < m_S/2$. From a direct comparison with the EFT expansion for $\cot \delta$

$$\cot \delta(k) = \sum_{\nu=0}^{\infty} [\cot \delta(k)]^{(\nu)} \left(\frac{Q}{M}\right)^\nu, \quad (134)$$

and the observation that the momentum k is a light scale, one arrives at the conclusion that $M = m_S/2$.

If one now considers the energy per nucleon, the perturbative contribution from V_S is given by

$$\frac{\delta E}{A} = \frac{\Omega}{2A} \int_{k_1, k_2 < k_F} \frac{d^3 \vec{k}_1}{(2\pi)^3} \frac{d^3 \vec{k}_2}{(2\pi)^3} \langle V_S \rangle, \quad (135)$$

with $\langle V_S \rangle$ denoting the projection of V_S into an antisymmetric two-body state and its sum on spin / isospin. The contribution to the energy per particle of this correction contains a term proportional to

$$\frac{\delta E}{A} \propto \log\left(1 + \frac{4k_F^2}{m_S^2}\right), \quad (136)$$

which has a branch cut at $k_F = \pm i(m_S/2)$. Thus, from this argument the EFT expansions for two-body scattering in powers of the external momentum k and the EOS in powers of k_F work in exactly the same way: they are expansions in k_F/M and k/M , where the breakdown scale M is identical, as originally argued in [44].

The literal identification of m_S with the rho meson mass ($m_\rho \approx 770$ MeV) implies $M = m_\rho/2 \approx 385$ MeV for two-body scattering and nuclear matter. This in turn leads to a breakdown density of $\rho_M \approx 3\rho_0$, with ρ_0 the equilibrium density of symmetric nuclear matter.

Though this breakdown scale is plausible, it might be erring on the conservative side. This argument, when

applied to pionless EFT, results in a breakdown scale of $M = m_\pi/2 \approx 70$ MeV. Common pionless EFT practice suggests $M = m_\pi$ instead, while the competing Bayesian analysis in [68] results in $M \approx 200$ MeV. And though there is a Bayesian analysis [69] that generates M close to $m_\pi/2$, it uses NDA instead of the power counting of pionless EFT. This indicates that $M = m_\pi/2$ (and hence $M = m_\rho/2$) might result in an underestimation of the actual breakdown scale.

Bayesian estimations in EFT-inspired potentials containing pions (but following NDA instead of the pionful EFT counting) yield $M \approx (400 - 600)$ MeV depending on the specific two-nucleon potential studied [70, 71]. This range is rather wide and when translated into nuclear matter leads to a breakdown density of $\rho_M \approx (3 - 12)\rho_0$. It is interesting to mention that the recent methodology of [72, 73] points to $M \approx (600 - 750)$ MeV, potentially leading to $\rho_M \approx (12 - 24)\rho_0$.

There is a different argument which comes from the observation that k_F^* is defined from what might be called the healing cutoff Λ^* . This implies that the hardest k_F^* around which the EOS can be expanded is determined by the hardest Λ^* that can be realistically chosen, which in turn is given by the appearance of the first pole (i.e. the first deeply bound state) in the running of the full, non-perturbative calculation of $C_0(\Lambda)$. That is, if $C_0(\Lambda)$ diverges at $\Lambda = \Lambda_B$ then $\Lambda^* < \Lambda_B$, from which the breakdown scale for k_F^* can be derived once the corresponding proportionality factor is included.

The exact location of Λ_B is not known because it depends on the full EFT potential for which the expansion becomes more and more expensive with each new order. If one includes the finite-range physics up to subleading TPE, then Λ_B sits typically around 500 MeV, give or take. For a sharp-cutoff the proportionality is given by $k_F^* = (2/\pi)(\Lambda^*/c_{0F})$ ($\approx 1.2136\Lambda^*$), which leads to $k_B \approx 600$ MeV for $\Lambda_B \approx 500$ MeV and a breakdown density of $\rho_M \approx (11 - 12)\rho_0$.

H. Three- and four-body forces

In symmetric nuclear matter, owing to the existence of four internal degrees of freedom, besides the already discussed 2-body forces there are also 3- and 4-body forces. For simplicity I will only consider density-dependent few-body forces

$$V_{3B} = \sum_{n \geq 0} D_{2n} k_F^{2n}, \quad (137)$$

$$V_{4B} = \sum_{n \geq 0} E_{2n} k_F^{2n}, \quad (138)$$

where D_{2n} , E_{2n} are the coupling constants. With these additions the EOS at tree level reads

$$\begin{aligned} \frac{E}{A} &= t\rho^{2/3} + c_0\rho + c_2\rho^{5/3} + \sum_{n \geq 2} c_{2n}\rho^{1+2n/3} \\ &+ d_0\rho^2 + d_2\rho^{8/3} + \sum_{n \geq 2} d_{2n}\rho^{2+2n/3} \\ &+ e_0\rho^3 + e_2\rho^{11/3} + \sum_{n \geq 2} e_{2n}\rho^{3+2n/3}, \end{aligned} \quad (139)$$

where the d_{2n} and e_{2n} coefficients are proportional to the D_{2n} and E_{2n} couplings.

If one momentarily ignores the interference with the two-body forces (which will be important), the loop corrections to the 3-body contributions is simply given by the first iteration of the 3-body force

$$\begin{aligned} \frac{\delta E_3}{A} &\propto \frac{1}{\rho} \int_{k_1, k_2, k_3 < k_F} \frac{d^3 \vec{k}_1}{(2\pi)^3} \frac{d^3 \vec{k}_2}{(2\pi)^3} \frac{d^3 \vec{k}_3}{(2\pi)^3} \\ &\times \int \frac{d^3 \vec{p}_{12}'}{(2\pi)^3} \frac{d^3 \vec{p}_3'}{(2\pi)^3} \frac{|V_{3B}|^2}{e_{123}} Q_F \end{aligned} \quad (140)$$

with the energy denominator

$$\begin{aligned} e_{123} &= \sum_i \frac{\vec{k}_i^2}{2m_N} - \sum_i \frac{\vec{k}'_i{}^2}{2m_N} \\ &= \frac{p_{12}^2}{m_N} + \frac{3p_3^2}{4m_N} - \frac{p'_{12}{}^2}{m_N} - \frac{3p_3'^2}{4m_N}, \end{aligned} \quad (141)$$

where the second line is written in terms of the Jacobi momenta. The projector Q_F is now defined as

$$Q_F = \theta(k'_1 - k_F) \theta(k'_2 - k_F) \theta(k'_3 - k_F), \quad (143)$$

with

$$\vec{k}'_1 = \frac{\vec{P}'}{3} - \frac{\vec{p}_3'}{2} + \vec{p}_{23}', \quad (144)$$

$$\vec{k}'_2 = \frac{\vec{P}'}{3} - \frac{\vec{p}_3'}{2} - \vec{p}_{23}', \quad (145)$$

$$\vec{k}'_3 = \frac{\vec{P}'}{3} + \vec{p}_3'. \quad (146)$$

Owing to momentum conservation, $\vec{P}' = \vec{P}$, with $\vec{P} = \vec{k}_1 + \vec{k}_2 + \vec{k}_3$ the total momentum of the three initial fermions in the sea.

The degree of divergence of this integral can be determined from defining a six dimensional momentum variable $p'^2 = p'_{12}{}^2 + \frac{3}{4}p_3'^2$, yielding

$$\begin{aligned} &\int_{\Lambda} \frac{d^3 \vec{p}_{12}'}{(2\pi)^3} \frac{d^3 \vec{p}_3'}{(2\pi)^3} \frac{|V_{3B}|^2}{e_{123}} Q_F \\ &\sim m_N |V_{3B}|^2 \int_{\Lambda} \frac{d^6 \vec{p}'}{(2\pi)^6} \frac{1}{p'^2} \\ &\sim m_N |V_{3B}|^2 \Lambda^4, \end{aligned} \quad (147)$$

where Λ is the cutoff (that has been directly applied to the six dimensional momentum). Naively, this implies that the iteration of the 3-body force diverges as

$$\frac{\delta E_3}{A} \propto m_N \Lambda^4 [D_0^2 + 2D_0 D_2 k_F^2 + \dots], \quad (148)$$

while for the 4-body force (by repeating similar arguments and assumptions) the divergence is

$$\frac{\delta E_4}{A} \propto m_N \Lambda^7 [E_0^2 + 2E_0 E_2 k_F^2 + \dots]. \quad (149)$$

The naive reading of this divergence structure suggests that the subset of couplings that is closed under loop corrections is composed by the lowest order A-body forces. Yet, this is but a conjecture and is far from proven: it only takes into account the leading divergence Λ^{3A-5} , which is followed by density-dependent divergences of the type $\Lambda^{3A-5-2n} k_F^{2n}$ that are much more difficult to handle if one wants to prove closure. This requires to take into account the interference with two-body forces, particularly in the 3-body case (as happens, for instance, in dilute systems [59], though there one goes from a divergence involving two-body forces to the inclusion of 3-body forces). After all, this contact appears from the necessity of preventing the Thomas collapse induced by the contact-range two-body forces.

For the specific case of the 3-body forces, the complete divergent structure of the 3-body loop actually is

$$\begin{aligned} \frac{\delta E_3}{A} &\propto m_N \left(c_4 \Lambda^4 + c_2 k_F^2 \Lambda^2 + c_0 k_F^4 \log \frac{\Lambda}{k_F} \right) \\ &\times [D_0^2 + 2D_0 D_2 k_F^2 + \dots], \end{aligned} \quad (150)$$

which is not renormalizable with the δD_0 correction to the 3-body coupling alone (where it is interesting to notice that the vacuum version of this problem has been already discussed in [74]). Here the inclusion of auxiliary δD_2 and δD_4 corrections (without the corresponding finite part) should in principle be able to absorb the k_F -dependent divergences.

Yet, a more satisfying solution might be found in the observation that the iteration of the two-body coupling C_0 is only suppressed when sandwiched and averaged between states in the Fermi sea. Within the D_0^2 loop it is thus perfectly possible to nest C_0 two-body loops, which (if not suppressed within internal loop lines) end up reproducing the in-medium 3-body wave function:

$$\begin{aligned} &\int_{\Lambda} \frac{d^3 \vec{p}_{12}'}{(2\pi)^3} \frac{d^3 \vec{p}_3'}{(2\pi)^3} \frac{|V_{3B}|^2}{e_{123}} Q_F \\ &\rightarrow \int_{\Lambda} \frac{d^3 \vec{p}_{12}'}{(2\pi)^3} \frac{d^3 \vec{p}_3'}{(2\pi)^3} |V_{3B}|^2 \Psi_{3F}(\vec{p}_{12}', \vec{p}_3'). \end{aligned} \quad (151)$$

Assuming that at short distances (or high momenta) the in-medium wave function behaves as the vacuum one, one

has

$$\Psi_{3F}(\vec{p}_{12}, \vec{p}_3) \rightarrow \frac{a(p_3)}{p_{12}^2 + \frac{3}{4} p_3^2}, \quad (152)$$

with

$$a(p_3) \rightarrow \frac{1}{p_3^2} \sin \left[s_0 \log \frac{p_3}{\Lambda_3} \right], \quad (153)$$

where $s_0 \approx 1.00624$ for a system of three identical particles in S-wave, and with Λ_3 a momentum scale that is fixed by the 3-body force (check [75–77] for further details). From this, the divergence structure might be schematically written as

$$\begin{aligned} & \int_{\Lambda} \frac{d^3 \vec{p}_{12}'}{(2\pi)^3} \frac{d^3 \vec{p}_3'}{(2\pi)^3} |V_{3B}|^2 \Psi_{3F}(\vec{p}_{12}', \vec{p}_3') \\ & \sim |V_{3B}|^2 \left(c_2 \Lambda^2 + c_0 k_F^2 \sin \left[s_0 \log \frac{\Lambda}{\Lambda_3} + \phi_3 \right] \right), \end{aligned} \quad (154)$$

with ϕ_3 a phase. Now the δD_0 correction is able to absorb the quadratic divergence, where the only loose end is the cutoff dependence originating from the oscillatory term, which is not divergent. Thus, though still far away from being a proof, this argument suggests that closure is a probable outcome for the lowest order 3-body forces.

Be it as it may, if one accepts the closure conjecture, one obtains the EOS:

$$\frac{E}{A} \Big|_{\text{closed}} = t\rho^{2/3} + c_0\rho + d_0\rho^2 + e_0\rho^3, \quad (155)$$

where it is important to stress that this is not necessarily the LO EOS, but a general candidate to the LO EOS. It is important to stress though that this is not the most general candidate for a LO EOS: as will be explained in Section IV, there are density-dependent terms that originate from integrating out intermediate range physics that have to be included in the EOS. These terms also make unnecessary the 3-body force in its role of avoiding the collapse of nuclear matter (though they do not prevent the inclusion of 3-body forces if they are still required by power counting arguments).

For illustrating the power counting of the 3- and 4-body contributions with a specific example, I will consider their scaling in pionless EFT [75–77]

$$D_0 \sim Q^{-4} \text{ (LO)} \quad \text{and} \quad E_0 \sim Q^{-6} \text{ (NLO)}, \quad (156)$$

where for the 4-body force I have followed its conjectured counting in [78]. The subleading 3- and 4-body forces inherit the scaling of their LO counterparts

$$D_{2n} \sim Q^{-4} \quad \text{and} \quad E_{2n} \sim Q^{-6}, \quad (157)$$

where the first of these scalings is a consequence of sandwiching the 3-body contact with the 3-body wave function (as done in [61]), while the second is the naive expectation once one considers that E_0 is already a perturbative correction (as normally they are all equally promoted). Meanwhile, the pure 3- and 4-body loops scale

as Q^4 and Q^7 (that is, the same power they diverge with). With this as the starting point, one ends up with

$$\frac{E_3}{A} = \underbrace{d_0 \rho^2}_{Q^2 \text{ (LO)}} + \underbrace{d_2 \rho^{8/3}}_{Q^4 \text{ (N}^2\text{LO)}} + \underbrace{d_4 \rho^{10/3}}_{Q^6 \text{ (N}^4\text{LO)}} + \dots \quad (158)$$

$$\frac{E_4}{A} = \underbrace{e_0 \rho^3}_{Q^3 \text{ (NLO)}} + \underbrace{e_2 \rho^{11/3}}_{Q^6 \text{ (N}^4\text{LO)}} + \underbrace{e_4 \rho^{14/3}}_{Q^8 \text{ (N}^7\text{LO)}} + \dots \quad (159)$$

for the derivative (or top-down) counting. For other countings the arguments are analogous, though in pionless EFT there is the open problem of how to count the 3- and 4-body contact-range forces (the consensus seems to be that they are not required up to NLO [79–81], though it has not been determined yet at which order they do appear).

IV. RENORMALIZATION GROUP AND DENSITY DEPENDENCE

The top-down EFT formulation of nuclear matter I have previously adopted might also be characterized as *vacuum-derived*. The starting point are the few-nucleon forces in the vacuum, which are then evolved into the infrared to derive power counting rules for the EOS.

Yet, a *medium-derived* EFT formulation is not only possible but necessary for uncovering infrared corrections to the EOS that are missed in the vacuum centered approach. By medium-derived I refer to the idea of introducing a cutoff in the G-matrix and then observing what type of counterterms or other correcting terms are forced if I impose cutoff independence. In the vacuum case — that is, if one derives the EFT from the requirement of a cutoff-independent T-matrix — this approach simply reproduces the derivative expansion of the contact-range interactions. In contrast, cutoff independence in nuclear matter leads to the appearance of new compensating terms explicitly depending on the density of the system. This includes terms that scale with a fractional powers of the Fermi momentum, which have been traditionally required to reproduce the compressibility of nuclear matter.

A. Compensating terms in the vacuum

If one considers first the vacuum, the starting point is the relation

$$T(E + i\epsilon) |\vec{p}\rangle = V |\Psi_{\vec{p}}^{\pm}\rangle, \quad (160)$$

which connects the two-body incoming and outgoing wave functions, $|\vec{p}\rangle$ and $|\Psi_{\vec{p}}^{\pm}\rangle$, by means of the T-matrix and the potential. For convenience it will be better to work with what is often referred to as the K-matrix, which is related to the T-matrix by

$$\frac{1}{K(E)} = \text{Re} \left[\frac{1}{T(E)} \right]. \quad (161)$$

If one projects into S-wave, the relation between the incoming and outgoing wave function now reads

$$K(E) |p\rangle = V |\Psi_p\rangle, \quad (162)$$

with

$$\langle r|p\rangle = \frac{\sin(pr)}{pr} \quad \text{and} \quad \langle r|\Psi_p\rangle = \frac{u_p(r)}{r}, \quad (163)$$

where $u_p(r)$ is the S-wave reduced wave function, defined with the asymptotic ($r \rightarrow \infty$) normalization

$$u_p(r) \rightarrow \frac{\sin(pr + \delta(p))}{p}, \quad (164)$$

with $\delta(p)$ the S-wave phase shift. If one now considers the on-shell K-matrix:

$$K(p) = \langle p|K(E = \frac{p^2}{m_N})|p\rangle = \frac{4\pi}{m_N} \frac{\tan \delta(p)}{q}, \quad (165)$$

then it can be expressed as the r-space integral

$$K(p) = 4\pi \int_0^\infty dr V(r) \frac{\sin(pr)}{p} u_p(r), \quad (166)$$

where the potential and reduced wave functions are the exact ones, which are usually unknown at short distances.

Now one may separate the integral in two parts by means of a cutoff

$$K(p) = 4\pi \int_{R_c}^\infty dr V(r) \frac{\sin(pr)}{p} u_p(r) + 4\pi \int_0^{R_c} dr V(r) \frac{\sin(pr)}{p} u_p(r), \quad (167)$$

which might be used as a tool to isolate the unknown physics at short distances. Within the second integral ($r < R_c$), it is in principle possible to expand the reduced incoming and outgoing wave functions in powers of the momentum

$$\frac{\sin(pr)}{p} = \sum_{n=0}^{\infty} (-1)^n \frac{p^{2n} r^{2n+1}}{(2n+1)!},$$

$$u_p(r) = \sum_{n=0}^{\infty} u_{2n}(r) p^{2n}, \quad (168)$$

which leads to the expansion

$$4\pi \int_0^{R_c} dr V(r) \frac{\sin(pr)}{p} u_p(r) = \sum_{n=0}^{\infty} v_{2n}(R_c) p^{2n}, \quad (169)$$

with $v_{2n}(R_c)$ basically representing moments of the potential $V(r)$ at short distances. Provided the potential is regular and has a finite range this expansion converges

at low momenta, in which case the full K-matrix can be perfectly recovered from the expansion

$$K(p) = \int_{R_c}^\infty dr V(r) \frac{\sin(pr)}{p} u_p(r) + \sum_{n=0}^{\infty} v_{2n}(R_c) p^{2n}. \quad (170)$$

This is expected to be equivalent to substituting the potential at distances $r < R_c$ by a series of contact-range terms

$$V(r) \rightarrow \sum_{n=0}^{\infty} C_{2n}(R_c) \delta_{2n}(r; R_c), \quad (171)$$

where $\delta_{2n}(r; R_c)$ is a regularization of a Dirac-delta involving $2n$ derivatives. They might be spatial or time derivatives, depending on whether one chooses momentum- or energy-dependent contact-range interactions, yet they have a clear Lagrangian interpretation.

The bottom-line is that by integrating out the short distance degrees of freedom one recovers the usual contact-range structure of non-relativistic EFTs. It is worth noting though that this formalism is non-perturbative in nature and thus not really suited to analyze power counting in general: it cleanly uncovers the lowest order contact-range interaction and its scaling, but it fails when applied to the higher order contacts, which are perturbative by virtue of being subleading. Yet, the present formalism is easily extended to the perturbative case. These issues will not be explained here though, but in Appendix C.

B. Compensating terms in the medium

With the G-matrix the argument is analogous, except for a few important differences. The first is the relation [38]

$$G(E) |\vec{p} \vec{P}\rangle = V |\Psi_{\vec{p}, \vec{P}}\rangle, \quad (172)$$

which connects the free and correlated (or in-medium) two-body wave functions, where now the dependence in the total momentum \vec{P} appears. The second difference is that there are no $i\epsilon$ factors if the two fermions are below the Fermi sea, which removes the intermediate step of defining a K-matrix equivalent. With this for S-waves one ends up with

$$G(p, P; k_F) = 4\pi \int_0^\infty dr V(r) \frac{\sin(pr)}{p} u_{p,P}(r; k_F), \quad (173)$$

where the reduced wave function is normalized as

$$u_{p,P}(r) \rightarrow \frac{\sin(pr)}{p}, \quad (174)$$

for $r \geq R^*$, with R^* the healing distance (which is inversely proportional to k_F). The expansion of the reduced in-medium wave function is now

$$u_{p,P}(r; k_F) = u_0(r) + P u_1(r) + p^2 u_{2A}(r) + P^2 u_{2B}(r) + \dots, \quad (175)$$

where the expansion now includes powers of P . This generates new terms in the expansion of the integral

$$\begin{aligned} 4\pi \int_0^{R_c} dr V(r) \frac{\sin(pr)}{p} u_{p,P}(r; k_F) \\ = v_0(R_c) + v_1(R_c) P \\ + v_{2A}(R_c) p^2 + v_{2B}(R_c) P^2 + \dots, \end{aligned} \quad (176)$$

that don't (and can't) appear in the vacuum Lagrangian: a two-body potential explicitly depending on P breaks Galilean invariance.

By separating the EOS in contributions above and below the cutoff scale and then explicitly considering the effect of these non-Lagrangian terms on the energy per particle, one finds:

$$\begin{aligned} \frac{E}{A} &= \frac{E}{A} \Big|_{r \geq R_c} + \frac{E}{A} \Big|_{r < R_c} \\ &= \frac{E}{A} \Big|_{r \geq R_c} + \sum_b c_n(R_c) k_F^{3+b}, \end{aligned} \quad (177)$$

where it is apparent that the non-Lagrangian terms manifest as density-dependence that can be directly included in the EOS without resort for the intermediate step of assuming the existence of density-dependent contact-range potentials. In fact, the new density-dependent terms often depend on powers of the Fermi momentum that do not appear at tree-level for normal contact-range interactions (this is the reason why the values of the sum index are not explicitly indicated in the formula above), which always involve an even number of derivatives.

Yet, density-dependent contacts are a really convenient bookkeeping device for reproducing the corrections to the EOS that originate from integrating out the short-range physics. This implies that these energy-dependent contact interactions are not actual contacts though and do not have to be iterated: provided they originate from terms that do not have a Lagrangian interpretation, they only make sense at tree level. The value of their couplings is still allowed to receive subleading order corrections, though. It is important to stress that energy-density dependent terms are still connected to (and can be in principle calculated from) few-nucleon forces, or more properly, BMF effects originating from these few-nucleon forces.

In terms of the EFT formalism, one might write the contact-range potential as the sum of two contributions, a *genuine* one and a *pseudo-potential*:

$$V_C = V_C^{\text{gen}} + V_C^{\text{pseudo}}, \quad (178)$$

where the genuine contribution might be either a momentum- or energy-expansion

$$V_C^{\text{gen}} = \sum_{n=0}^{\infty} C_{2n} \left(\frac{p^{2n} + p'^{2n}}{2} \right) \quad \text{or} \quad \sum_{n=0}^{\infty} C_{2n} k^{2n}, \quad (179)$$

while the pseudo-potential contribution is density-dependent

$$V_C^{\text{pseudo}} = \sum_b \tilde{C}_b k_F^b, \quad (180)$$

where the expansion index b is left unspecified as it depends on the details of the system. For distinction purposes, the couplings corresponding to the pseudo-potentials have been marked with a tilde. It is important to stress that the pseudo-potential contribution is not meant to be iterated, but only used at tree level instead.

This convention allows for a clear distinction between contributions originating from integrating out the two-body forces (genuine) or BMF effects (pseudo-potential). Nonetheless it might still be in principle possible to use a density-dependent representation for the genuine contact-range interaction for specific purposes. Particularly when they might be convenient, as in the previous discussions about the power counting of few-body forces in the EOS.

C. Density-dependent terms

Now I will consider the specific form of the in-medium reduced wave function at short distances and its relation with the power counting of density-dependent terms. The easiest case is that of a reduced wave function that is regular at the origin

$$u_{p,P}(r; k_F) = r + b_1 P r^2 + b_{2A} p^2 r^3 + b_{2B} P^2 r^3 + \dots, \quad (181)$$

where the normalization of the term proportional to r (equal to one) has been determined from the condition of converging to the free solution above the healing distance. In this case the LO interaction is a momentum- and energy-independent contact-range potential, which is also density-independent. This reproduces the vacuum power counting of a theory in which the scattering length is small.

Notice that there are density-dependent corrections, but they are subleading. In particular the BMF effects generating these density dependent corrections are perturbative themselves. As a consequence they are reproducible in terms of the iterations of the usual (or genuine) EFT potential and no pseudo-potential contribution is actually required.

The next case is when the reduced wave function is irregular at the origin

$$u_{p,P}(r; k_F) = \mathcal{N}(k_F) [1 + b_1 P r + \dots], \quad (182)$$

where now it is necessary to include a normalization factor $\mathcal{N}(k_F)$. The scaling of the normalization factor with k_F is easy to determine from the condition that the wave function heals around $k_F r \sim 1$:

$$\begin{aligned} u_{p,P}(r \sim \frac{1}{k_F}; k_F) &\sim \frac{1}{p} \sin\left(\frac{p}{k_F}\right) \\ &\sim \frac{1}{k_F} - \frac{p^3}{6 k_F^2} + \mathcal{O}\left(\frac{p^5}{k_F^4}\right), \end{aligned} \quad (183)$$

where in the second line one expands in powers of p/k_F . This leads to

$$\mathcal{N}(k_F) \sim \frac{1}{k_F}, \quad (184)$$

which implies the existence of a correction term that explicitly depends on k_F , that is:

$$\begin{aligned} 4\pi \int_0^{R_c} dr V(r) \frac{\sin(pr)}{p} u_{p,P}(r; k_F) \\ = \frac{v_{-1}(R_c)}{k_F} + v_0(R_c) + \dots \end{aligned} \quad (185)$$

Equivalently, if one relies on density-dependent pseudo contact-range interactions, the LO contact-range potential will contain a genuine and pseudo-potential contribution

$$V_C^{\text{LO}} = C_0 + \frac{\tilde{C}_{-1}}{k_F}. \quad (186)$$

With this contact the LO EOS reads:

$$\frac{E}{A} \Big|_{\text{LO}} = t \rho^{2/3} + c_{-1} \rho^{2/3} + c_0 \rho, \quad (187)$$

where the c_{-1} term originating from the density-dependent pseudo contact displays the same density-dependence as the kinetic term. This is not arbitrary: this term is basically there because the irregular wave function corresponds to expanding around the unitary limit. This in turn requires a contribution to reproduce the Bertsch parameter [82], which is a BMF effect as it requires the full iteration of the LO vacuum contact.

D. Fractional powers of the Fermi momentum

Finally, I consider the case when the reduced wave function behaves as r^a with the exponent a not necessarily integer:

$$u_{p,P}(r) = \mathcal{N}(k_F) [r^a f_0(Qr) + b_1 P r^{a+1} f_1(Qr) + \dots], \quad (188)$$

where $f_0(x)$, $f_1(x)$ are oscillatory functions of order one, usually taking the form of a trigonometric (e.g. sine, cosine) function with arguments $1/x^{2a-1}$ (and Q representing a light scale related to the strength of the potential generating the wave function). Matching to the free wave function at $k_F r \sim 1$, the normalization factor of this wave function scales as

$$\mathcal{N}(k_F) \propto k_F^{a-1}, \quad (189)$$

leading to a density-dependent correction of the type

$$V_C^{\text{pseudo}} = \tilde{C}_{a-1} k_F^{a-1}. \quad (190)$$

This type of reduced wave function appears as the non-perturbative solution of inverse power-law attractive singular potentials, where for $V(r) \propto -1/r^n$ the exponent of the wave function is $a = n/4$. That is, one ends up with a density dependence involving a fractional exponent of the Fermi momentum.

If the behavior of the wave function below the healing distance is driven by subleading TPE ($n = 6$), which is by far the strongest contribution to the chiral potential at intermediate distances, the density dependent term will be proportional to $k_F^{1/2}$ or $\rho^{1/6}$. This coincides with one of the most common exponents appearing in density-dependent Skyrme forces. In this case at LO the effective interaction (contact plus pseudo contact) is

$$V_C^{\text{LO}} = C_0 + \tilde{C}_{1/2} k_F^{1/2}, \quad (191)$$

and the EOS reads

$$\frac{E}{A} \Big|_{\text{LO}} = t \rho^{2/3} + c_0 \rho + c_{1/2} \rho^{1+1/6}, \quad (192)$$

where it is important to keep in mind that the fractional density dependence does not come from a genuine contact-range potential, but is instead the result of integrating out the BMF effects coming from subleading TPE, which can be encoded in a density-dependent pseudo-potential.

This is a really exciting result. First, it provides a simple explanation for the t_3 density-dependent term typically appearing in Skyrme forces:

$$\delta V_{\text{Skyrme}} = \frac{1}{6} t_3 (1 + x_3 P_\sigma) \rho^\alpha, \quad (193)$$

where t_3 is the coupling, x_3 a parameter and $P_\sigma = (1 + \vec{\sigma}_1 \cdot \vec{\sigma}_2)/2$ the spin-exchange operator (with eigenvalues -1 and +1 for the singlet and triplet, respectively). Second, it also explains one of its most usual exponents, $\alpha = 1/6$. Third, by not associating the microscopic explanation of this term with a three-body force, but with a isoscalar and central two-body force — which happens to be the strongest medium-range ($1 \leq m_\pi r \leq 2$, with m_π the pion mass) contribution to the EFT potential by far — there is no mystery as to why this term is usually included in neutron matter calculations.

There are caveats as well: for starters, while the exponent in the Fermi momentum of the pseudo contact depends explicitly on the behavior of the wave function at distances that are formally long-range, the truth is that the scale separation in nuclear EFT is not particularly clean. That is, the $1 \leq m_\pi r \leq 2$ distance range which determines the fractional exponents are what could be denoted as *intermediate scales*, sitting uncomfortably in between the long- and short-range scales of the two-nucleon system. Thus, a certain degree of skepticism is justified regarding whether the reduced wave function really displays the $r^{3/2}$ power-law dependence required to explain the $\alpha = 1/6$ exponent.

Yet, predictions derived from subleading TPE alone tend to work well. For instance, the singlet and triplet two-nucleon phase shifts can be effectively described in terms of *chiral van der Waals forces* [83], which refer to the chiral limit ($m_\pi \rightarrow 0$) of subleading TPE.

Besides, this explanation requires that it should be possible to formulate an EFT in which subleading two-pion exchange is a LO effect. This idea was considered a long time ago [84], mostly as a pathology, where only recently has this alternative EFT expansion been explicitly shown to be a viable counting [85] (a more intuitive explanation of non-perturbative TPE in the singlet can be found in [86], though it does not explore the EFT expansion resulting from this choice). Indeed this expansion works perfectly well in two-nucleon scattering, outperforming more conservative EFT expansions in the singlet. But it remains unclear whether non-perturbatively renormalized subleading TPE can by itself generate saturation. While traditionally saturation requires the inclusion of three-nucleon forces, it is also true that renormalized OPE is able to saturate at cutoffs $\Lambda \gtrsim 1$ GeV [87], though the resulting saturation properties are far from ideal. Thus, it would be really interesting to know what happens with renormalized TPE and how much it improves over renormalized OPE.

V. DISCUSSION AND CONCLUSIONS

In this manuscript, I have considered the EFT description of nuclear matter. The observation underlying the present analysis is the special role of the healing distance in the infrared RG evolution of contact-range couplings in nuclear matter. The idea is that as the two-nucleon wave function evolves into a free wave function at interparticle separations larger than the healing distance, the running of the contact-range couplings essentially freezes. The resulting EFT description is thus different than in the vacuum: naively, couplings that do not run are expected to be perturbative. This intuition has been explicitly confirmed from analyzing the G-matrix and its corresponding contribution to the energy per nucleon in a contact-range theory, where loops happen to be suppressed in the medium.

The previous analysis relies however on knowing the

running of the coupling constants in nuclear matter at finite density, which is not always the case. Yet, this is not a requirement and one might as well use the vacuum running of the couplings at the cutoff Λ^* at which they are expected to freeze at a given density. This results in a power counting in which the loop integrals in nuclear matter are counted as $(k_F^* - k_F)$, instead of the usual Q , where k_F^* is proportional to Λ^* . This is interesting for the following reasons:

- (i) Independently of whether one is dealing with vacuum or nuclear matter, loops formally scale as Q (because $k_F^* - k_F$ is after all a light scale).
- (ii) Yet there is a density (of our choosing) for which loop corrections vanish, thus explaining why the LO couplings do not have to be iterated in nuclear matter. That is, they only enter at tree level in the LO EOS, at least in the vicinity of k_F^* , which is where the EFT expansion of the EOS is optimized.

Probably a good choice for k_F^* is the Fermi momentum reproducing the equilibrium density of symmetric nuclear matter. Of course this expansion will not work far from k_F^* , yet the EOS is by itself not an observable: what matters is either its equilibrium properties (density, energy per nucleon, compressibility) or the observable properties of the system for which the EOS is an input (e.g. the maximum mass of a neutron star). Besides, once the initial expansion around a given k_F^* fails, there is always the possibility of redefining the EFT expansion of the EOS around a second Fermi momentum $k_F'^*$.

The power counting of the contact-range couplings in nuclear matter is in principle inherited from the vacuum. Thus one is free to choose among the different countings available in the few-nucleon system. Yet, there is a caveat: if one wants loop contributions to be finite then it is necessary to include auxiliary or redundant counterterms, that is, counterterms that do not carry physical information but are there to remove residual cutoff dependence (a more detailed explanation may be found in [63]). The reason is that the EFT expansion of nuclear matter is perturbative, which implies that the matching with the RG evolution of few-body forces happens at soft cutoffs. If one expands around the soft cutoff limit, the (originally harmless) residual cutoff dependence manifests as divergences. If the auxiliary counterterms absorbing the residual cutoff dependence are there in the first place, the divergences are removed. But if the auxiliary counterterms are not present, which is what happens with most EFT expansions in the few-body sector, then new counterterms have to be introduced to cure the divergences. In general, if this is the case, one is effectively forced to add new parameters to the EFT description of nuclear matter. The reason is that without the auxiliary counterterms there is no right guess about the size of the finite part of the new counterterms.

Thus there are two approaches to the power counting of nuclear matter

- (a) A top-down approach, where power counting coincides with that of the vacuum at all orders, but which requires the inclusion of auxiliary counterterms not encoding physical information.
- (b) A bottom-up approach, where power counting is eventually modified from the necessity of absorbing divergences that appear in many-body perturbation theory (even though these are divergences that vanish after resummation).

Both approaches are formally equivalent once all many-body perturbative corrections are included, and hence their difference is practical rather than theoretical. But if one is interested in deriving the nuclear matter EOS directly from few-nucleon forces, it will be necessary to extend the concept of *improved actions* [64–66] (equivalent to the idea of auxiliary counterterms [63]) from LO to subleading orders.

Besides the contact-range interactions already appearing in the EFT expansion of the two-nucleon system, their infrared RG evolution at finite density (which involves the analysis of the G-matrix) implies the existence of new compensating or correcting terms that appear in nuclear matter. These are density-dependent terms that might be directly included in the EOS or indirectly by means of a contact-range pseudo-potential. By a pseudo-potential it is meant a term formally identical to a contact-range potential except for the fact that it should not be iterated (as it does not represent a real two-body interaction). This provides a clean explanation of the density-dependent terms usually appearing in the Skyrme and Gogny interactions [11, 12]. In particular the RG evolution of chiral TPE in the infrared explains one of the most typical exponents for the first density-dependent term (the t_3 term) in Skyrme.

The breakdown scale of the EFT expansion of nuclear matter is in principle identical to that of the two-nucleon sector, as previously argued in the literature [44]. The reason is that the T- and G-matrices share the same short-range behavior, and thus lead to the same breakdown scale once the center-of-mass momentum k is substituted with the Fermi momentum k_F . Usual estimations of the breakdown scale of two-nucleon scattering lie in the $M \approx (400 - 600)$ MeV range [70–73], suggesting a *breakdown density* of

$$\rho_M \approx (3 - 12) \rho_0, \quad (194)$$

with ρ_0 the equilibrium density of symmetric nuclear matter. One might distinguish though between *intrinsic* and *extrinsic* breakdown scales, where the first refers to the convergence of the perturbative expansion of finite-range forces (the most evident example being KSW [39, 40] and its N²LO failure [67]), while the second to the genuine limitations coming from short-range physics outside the control of the EFT. It might happen that the perturbative expansion of OPE, which is the limiting factor for the convergence of KSW [67], is

more convergent at finite densities than in the vacuum thus making KSW a viable counting in nuclear matter. Yet, this is but a conjecture at this point: elucidating this question will require adapting current investigations about the perturbativeness of OPE [88, 89] to the finite density case.

The LO contact-range potential and pseudo-potential depend partly on the choice of a power counting (pionless [39, 40], KSW [47, 48], pionful [51–58]) and partly on the choices of which BMF effects to integrate out and include in the pseudo-potential. For a KSW-type counting (S-wave contacts at LO, subleading pions) and a pseudo-potential derived from the two-pion exchange wave function, the LO EOS is the one obtained with the t_0 - t_3 subset of the Skyrme interaction. This coincides with the findings from the Orsay group [21–24], though there is a crucial difference in regards to the status of the density dependent term, which in the present approach is a pseudo-potential. In this regard it will be really interesting to recalculate the NLO EOS in the framework of the Orsay group with the pseudo-potential reinterpretation of the t_3 term, which will simplify the calculations.

If the starting point is pionful EFT instead, where OPE is leading and there is at least one LO P-wave contact-range potential, the LO EOS reads instead:

$$\begin{aligned} \frac{E}{A} \Big|_{\text{LO}} &= t \rho^{2/3} + c_0 \rho + c_2 \rho^{1+2/3} + c_{1/2} \rho^{1+1/6} \\ &+ \frac{E}{A} \Big|_{\text{OPE}}, \end{aligned} \quad (195)$$

with the origin of the c_2 coefficient being now the P-wave contribution and where the OPE contribution in the second line (not written down explicitly here) has been calculated for instance in [90, 91]. (which also includes expressions for the iteration of OPE, necessary at NLO and beyond). Though this pionful EOS has a more complicated subleading structure than the t_0 - t_3 subset, it will be interesting to adapt the formalism of [21–25] to it and explore its NLO predictions.

To summarize, the infrared RG evolution of nuclear matter differs from that of few-body forces in the vacuum owing to the appearance of a new long distance scale (the healing scale). This leads to its own low energy EFT expansion, in which forces that were non-perturbative in the vacuum become perturbative at finite densities. In principle the RG evolution of the couplings in nuclear matter requires the couplings to explicitly depend on the Fermi momentum (and thus on density). Yet this requirement can be waived, in which case one ends up with an expansion that is optimized at a particular density of one's own choice. This expansion also involves the inclusion of density-dependent terms in the EOS that might in turn be conveniently represented by a density-dependent pseudo-potential. The lowest-order description of nuclear matter coincides with certain subsets of the Skyrme interaction already identified in the literature [21–25], though it might contain pionic contributions not present in Skyrme depending on the choice of a power

counting.

ACKNOWLEDGMENTS

I would like to thank Ludovic Bonneau for discussions and C.-J. (Jerry) Yang for discussions and a careful reading of the manuscript.

Appendix A: Expansion of the G-matrix

Here I consider the calculation of the G-matrix for a contact-range theory at the lowest order and its expansion in the infrared. This is necessary for a detailed understanding of the scaling properties of the loop corrections in nuclear matter.

1. G-matrix for a contact-range interaction

In the vacuum the on-shell T-matrix for a momentum- and energy-independent contact-range potential is

$$T(p) = \frac{1}{\frac{1}{C_0(\Lambda)} - I_0(p; \Lambda)}, \quad (\text{A1})$$

where $p = \sqrt{M_N E}$, with E the center-of-mass energy and I_0 the loop function, which is given by

$$I_0(p; \Lambda) = \int_{\Lambda} \frac{d^3 \vec{q}}{(2\pi)^3} \frac{1}{E - \frac{q^2}{m_N}}, \quad (\text{A2})$$

where the subscript Λ indicates that the integral is regularized. The exact form of I_0 depends on the choice of the regulator. If one regularizes with PDS, one obtains

$$I_0^{\text{PDS}}(p; \Lambda) = -\frac{m_N}{4\pi} (\Lambda + ik), \quad (\text{A3})$$

for the $E + i\epsilon$ prescription, where Λ is the PDS regularization (or renormalization) scale. From the condition of reproducing the scattering length a_0 (or, equivalently, the on-shell T-matrix at $p = 0$), one obtains the well-known running

$$\frac{1}{C_0^{\text{PDS}}(\Lambda)} = \frac{m_N}{4\pi} \left(\frac{1}{a_0} - \Lambda \right). \quad (\text{A4})$$

In the medium the G-matrix for a contact-range interaction is structurally identical to the T-matrix in the vacuum, that is:

$$G(p, P, k_F) = \frac{1}{\frac{1}{C_0(\Lambda)} - I_{0F}(p, P, k_F; \Lambda)}, \quad (\text{A5})$$

where the most obvious difference is that the loop integral now depends not only on the relative momentum p , but

also on the total and Fermi momenta, P and k_F . The loop integral reads

$$\begin{aligned} I_{0F}(p, P, k_F; \Lambda) &= \int_{\Lambda} \frac{d^3 q}{(2\pi)^3} \frac{Q_F}{E - \frac{q^2}{m_N}} \\ &= \int_{\Lambda} \frac{d^3 q}{(2\pi)^3} \frac{\theta(q_1 - k_F) \theta(q_2 - k_F)}{E - \frac{q^2}{m_N}}, \end{aligned} \quad (\text{A6})$$

with the subscript Λ again indicating regularization, and where in the second line the form of the projector Q_F is written explicitly, with

$$\vec{q}_1 = \frac{\vec{P}}{2} + \vec{q} \quad \text{and} \quad \vec{q}_2 = \frac{\vec{P}}{2} - \vec{q}, \quad (\text{A7})$$

the momentum of each of the two fermions in the loop. If one chooses a regularization that depends only on the relative momentum q , then the angular part of the integral is independent of the specific details of this regulator, in which case the loop integral can be written as

$$\begin{aligned} I_{0F}(p, P, k_F; \Lambda) &= \frac{m_N}{2\pi^2} \left[\int_{\sqrt{k_F^2 - P^2/4}}^{k_F + P/2} dq \left(\frac{P^2/4 + q^2 - k_F^2}{Pq} \right) \right. \\ &\quad \left. + \int_{k_F + P/2}^{\infty} dq \right] \frac{q^2}{p^2 - q^2} g\left(\frac{q}{\Lambda}\right), \end{aligned} \quad (\text{A8})$$

with $g(x)$ the regulator function. For a typical separable regulator, that is:

$$\langle p' | V_C | p \rangle = C_0(\Lambda) f\left(\frac{p'}{\Lambda}\right) f\left(\frac{p}{\Lambda}\right), \quad (\text{A9})$$

one has $g(x) = f^2(x)$. Besides, if the two particles are below the Fermi sea there is no need for the $i\epsilon$ prescription and the integral is real.

In PDS the loop integral can be divided into two parts, one that depends on the regularization scale Λ and one that does not:

$$I_{0F}^{\text{PDS}}(p, P, k_F; \Lambda) = -\frac{m_N}{4\pi} \Lambda + I_{0F}^{\text{reg}}(p, P, k_F), \quad (\text{A10})$$

where the scale-independent (or regular) piece can be further decomposed into

$$I_{0F}^{\text{reg}}(p, P, k_F) = I_{0Fa}(p, P, k_F) + I_{0Fb}(p, P, k_F), \quad (\text{A11})$$

with

$$\begin{aligned} I_{0Fa}(p, P, k_F) &= -\frac{m_N}{16\pi^2 P} \left[2P(2k_F + P) + \right. \\ &\quad \left. 4(k_F^2 - P^2/4 - p^2) \log \left(\frac{k_F^2 - P^2/4 - p^2}{(k_F + P/2)^2 - p^2} \right) \right], \end{aligned} \quad (\text{A12})$$

$$\begin{aligned} I_{0Fb}(p, P, k_F) &= \frac{m_N}{2\pi^2} (2k_F + P) \left[\right. \\ &\quad \left. 1 - \frac{p}{k_F + P/2} \operatorname{atanh} \left(\frac{p}{k_F + P/2} \right) \right], \end{aligned} \quad (\text{A13})$$

where they correspond to the two integration brackets in Eq. (A8), that is, from $q = \sqrt{k_F^2 - P^2/2}$ to $k_F + P/2$ for I_{0Fa} and from $q = k_F + P/2$ to infinity for I_{0Fb} .

With the previously defined scale-independent part of the loop integral, I_{0F}^{reg} , the calculation of the G-matrix in PDS reads

$$G(p, P, k_F) = \frac{4\pi}{m_N} \frac{1}{\frac{1}{a_0} - \frac{4\pi}{m_N} I_{0F}^{\text{reg}}}, \quad (\text{A14})$$

where the running of $C_0(\Lambda)$ has been taken from the vacuum case, Eq. (A4).

For a separable regulator the form of the loop integral follows the pattern:

$$I_{0F} = -\frac{m_N}{4\pi} c_r \Lambda + I_{0F}^{\text{reg}} + I_{0F}^{\text{res}} \quad (\text{A15})$$

where c_r is a regulator-dependent number, I_{0F}^{reg} the regular part of the loop integral, and I_{0F}^{res} a contribution only containing the residual cutoff dependence. The constant c_r is given by

$$c_r = \frac{2}{\pi} \int_0^\infty f^2(x) dx, \quad (\text{A16})$$

where for a sharp-cutoff — that is, $f(x) = \theta(1-x)$ — this numerical factor is $c_r = 2/\pi$. The part of the loop integral encoding the residual cutoff dependence can be written as

$$\begin{aligned} I_{0F}^{\text{res}}(p, P, k_F; \Lambda) &= \frac{m_N}{2\pi^2} \left[\int_{\sqrt{k_F^2 - P^2/4}}^{k_F + P/2} dq \left(\frac{P^2/4 + q^2 - k_F^2}{Pq} \right) \frac{q^2}{p^2 - q^2} \right. \\ &\quad \left. + \int_0^{k_F + P/2} dq \right] \left(f^2\left(\frac{q}{\Lambda}\right) - 1 \right), \end{aligned} \quad (\text{A17})$$

and, while simple in the $\Lambda \gg k_F$ limit (where it scales as $\mathcal{O}(\Lambda^{-1})$), it might become really involved for $\Lambda \lesssim k_F$.

With the previous components, the G-matrix for a separable regulator reads

$$G(p, P, k_F; \Lambda) = \frac{4\pi}{m_N} \frac{1}{\frac{1}{a_0} - \frac{4\pi}{m_N} (I_{0F}^{\text{reg}} + I_{0F}^{\text{res}})}, \quad (\text{A18})$$

where the $C_0(\Lambda)$ from which it has been calculated is given by

$$\frac{1}{C_0(\Lambda)} = \frac{m_N}{4\pi} \left(\frac{1}{a_0} - c_r \Lambda \right). \quad (\text{A19})$$

Independently of the regulator choice, the $\Lambda \rightarrow \infty$ limit of this G-matrix reproduces the result of Eq. (A14).

2. The G-matrix with a delta-shell regulator

The calculation of the G-matrix in r-space is not entirely trivial. The reason lies in the required set of techniques, which is very different from the more familiar methods used in the p-space case.

In particular I will derive the G-matrix from the form of the in-medium wave function, where the starting point is the (S-wave) Bethe-Goldstone equation

$$\Psi_{p,P}(r) = j_0(pr) + \int d^3\vec{r}' K_0(|\vec{r} - \vec{r}'|) V(\vec{r}') \Psi_{p,P}(r'), \quad (\text{A20})$$

with $\Psi_{p,P}$ the wave function, $j_0(x) = \sin x/x$ the spherical Bessel function, and with the in-medium propagator K_0 given by

$$K_0(r) = \int \frac{d^3\vec{q}}{(2\pi)^3} \frac{m_N}{p^2 - q^2} e^{i\vec{q}\cdot\vec{r}} \theta(q_1 - k_F) \theta(q_2 - k_F), \quad (\text{A21})$$

which can be rewritten as

$$\begin{aligned} K_0(r) &= \frac{m_N}{2\pi^2} \left[\int_{\sqrt{k_F^2 - P^2/4}}^{k_F + P/2} q^2 dq \left(\frac{P^2/4 + q^2 - k_F^2}{Pq} \right) \right. \\ &\quad \left. + \int_{k_F + P/2}^\infty q^2 dq \right] \frac{q^2}{p^2 - q^2} \frac{\sin(qr)}{qr}. \end{aligned} \quad (\text{A22})$$

It is worth noting that there is a closed form solution for $K_0(r)$, though it is rather unwieldy and will not be written down here.

If one regularizes the contact-range potential with a delta-shell

$$V_C(\vec{r}) = C_0(R_c) \frac{\delta(r - R_c)}{4\pi R_c^2}, \quad (\text{A23})$$

then it is useful to define the regularized in-medium propagator as

$$K_0(r; R_c) = \int_0^\infty dx \delta(x - R_c) \int \frac{d^2\hat{x}}{4\pi} K(|\vec{r} - \vec{x}|). \quad (\text{A24})$$

For $r = R_c$ the calculation simplifies to

$$\begin{aligned} K_0(R_c; R_c) &= \int_{-1}^{+1} \frac{du}{2} K_0(R_c \sqrt{2 - 2u}) \\ &= \frac{1}{2} \int_0^2 y dy K_0(R_c y), \end{aligned} \quad (\text{A25})$$

with the second line (which is the result of a change of variable) being particularly easy to calculate.

In the $R_c \rightarrow 0$ limit the evaluation of $K_0(R_c; R_c)$ complies with the expectation of a linear divergence plus a regular contribution that already appeared in Eq. (A10) for the p-space calculation:

$$K_0(R_c; R_c) = -\frac{m_N}{2\pi^2} \frac{1}{R_c} + I_{0F}^{\text{ref}} + \mathcal{O}(R_c), \quad (\text{A26})$$

with $I_{0F}^{\text{ref}} = I_{0Fa} + I_{0Fb}$ as written in Eqs. (A11-A13), from which it is apparent that $K_0(R_c; R_c)$ is simply the loop function in r-space.

For finding the G-matrix, one first notices that the Bethe-Goldstone equation for a delta-shell can be rewritten as

$$\begin{aligned}\Psi_{p,P}(r) &= j_0(pr) + C_0(R_c) \Psi_{p,P}(R_c) K_0(r; R_c) \\ &= j_0(pr) + \frac{j_0(pR_c) K_0(r; R_c)}{\frac{1}{C_0(R_c)} - K_0(R_c; R_c)},\end{aligned}\quad (\text{A27})$$

where the denominator in the second line seems to be the G-matrix. This identification has to be proven though, for which one might consider Eq. (17), which after taking matrix elements reads

$$\begin{aligned}\Psi_{p,P}(r) &= j_0(pr) \\ &+ \int \frac{d^2\hat{r}}{4\pi} \int \frac{d^2\hat{p}}{4\pi} \langle \vec{r} | \frac{Q_F}{E - H_0} G(E) | \vec{p} \rangle,\end{aligned}\quad (\text{A28})$$

where the angular integrals are there to ensure the projection into the S-wave. Then, if one takes into account that in p-space the delta-shell potential of Eq. (A23) is separable:

$$\langle p' | V_C | p \rangle = j_0(p'R_c) C_0(R_c) j_0(pR_c), \quad (\text{A29})$$

then the matrix elements of the G-matrix are

$$\langle p' | G(E) | p \rangle = j_0(p'R_c) G(E; R_c) j_0(pR_c), \quad (\text{A30})$$

where I have used the same symbol G for the operator and the part of its evaluation that does not depend on the form factor (they are easily distinguishable by the context). With this, it follows that

$$\begin{aligned}\int \frac{d^2\hat{r}}{4\pi} \int \frac{d^2\hat{p}}{4\pi} \langle \vec{r} | \frac{Q_F}{E - H_0} G(E) | \vec{p} \rangle \\ = G(E; R_c) j_0(pR_c) \int \frac{d^3\vec{q}}{(2\pi)^3} \frac{Q_F}{E - \frac{q^2}{m_N}} j_0(qR_c),\end{aligned}\quad (\text{A31})$$

which is not very revealing by itself until one uses the relation

$$j_0(qR_c) = \int d^3\vec{x} e^{-i\vec{q}\cdot\vec{x}} \frac{\delta(x - R_c)}{4\pi R_c^2}, \quad (\text{A32})$$

from which one arrives at

$$\begin{aligned}\int \frac{d^2\hat{r}}{4\pi} \int \frac{d^2\hat{p}}{4\pi} \langle \vec{r} | \frac{Q_F}{E - H_0} G(E) | \vec{p} \rangle \\ = G(E; R_c) j_0(pR_c) K_0(r; R_c),\end{aligned}\quad (\text{A33})$$

or, equivalently:

$$\Psi_{p,P}(r) = j_0(pr) + j_0(pR_c) G(E; R_c) K_0(r; R_c). \quad (\text{A34})$$

From this, the G-matrix ends up being

$$G(E; R_c) = \frac{1}{\frac{1}{C_0(R_c)} - K_0(R_c; R_c)}, \quad (\text{A35})$$

with its $R_c \rightarrow 0$ limit given by Eq. (A14).

3. In-medium renormalization of the G-matrix

At zero external momenta ($p = P = 0$) the G-matrix reads

$$G(0, 0, k_F) = \frac{4\pi}{m_N} \frac{1}{\frac{1}{a_0} - \frac{2}{\pi} k_F}. \quad (\text{A36})$$

This limit provides a different renormalization condition for the contact-range coupling. In this case the G-matrix is calculated as usual

$$G(p, P, k_F; \Lambda) = \frac{1}{\frac{1}{C_{0F}(\Lambda)} - I_{0F}(p, P, k_F; \Lambda)}, \quad (\text{A37})$$

but with $C_{0F}(\Lambda)$ determined from the condition of reproducing $G(0, 0, k_F)$, which is why C_{0F} is referred to as the in-medium coupling. That is, one is not required to calibrate the coupling to the $p = 0$ limit of the T-matrix. Yet, both renormalization conditions lead to the same G-matrix in the $\Lambda \rightarrow \infty$ ($R_c \rightarrow 0$) limit.

For a sharp cutoff in momentum space one has

$$\begin{aligned}I_{0F}(0, 0, k_F; \Lambda) &= -\frac{m_N}{2\pi^2} \int_{k_F}^{\Lambda} dq \\ &= -\frac{m_N}{2\pi^2} (\Lambda - k_F) \theta(\Lambda - k_F),\end{aligned}\quad (\text{A38})$$

and by setting the coupling to reproduce $G(0, 0, k_F)$ one obtains the $C_{0F}(\Lambda)$ of Eq. (64).

In r-space at $p = P = 0$ the propagator K_0 reads

$$\begin{aligned}K_0(r) &= -\frac{m_N}{2\pi^2} \int_{k_F}^{\infty} \frac{\sin(qr)}{qr} \\ &= -\frac{m_N}{2\pi^2} \frac{1}{r} \left(\frac{\pi}{2} - \text{Si}(k_F r) \right),\end{aligned}\quad (\text{A39})$$

which for a delta-shell regulator leads to the $K_0(r; R_c)$ of Eq. (27), from which the wave function in Eq. (30) follows and thus the running of the $C_{0F}(R_c)$ coupling of Eq. (32).

Finally, for PDS there is no difference for the coupling independently of whether the renormalization condition is given by the $p = 0$ T-matrix or the $p = P = 0$ G-matrix. The reason is that PDS regularization is not sensitive to the existence of the Fermi momentum as a low energy scale that impacts the behavior of loops.

4. The G-matrix in the infrared

If one now rewrites the G-matrix as

$$G(p, P, k_F) = \frac{4\pi}{m_N} \frac{1}{\frac{1}{a_0} - \frac{2}{\pi} k_F - \frac{4\pi}{m_N} \left(I_{0F}^{\text{reg}} - \frac{m_N}{2\pi^2} k_F \right)}, \quad (\text{A40})$$

then, at low external momenta, it is possible to expand it in inverse powers of $(\frac{1}{a_0} - \frac{2}{\pi} k_F)$

$$\begin{aligned} G(p, P, k_F) &= \frac{4\pi}{m_N} \frac{1}{\frac{1}{a_0} - \frac{2}{\pi} k_F} \\ &\times \sum_{n=0}^{\infty} \left[\frac{4\pi}{m_N} \frac{1}{\frac{1}{a_0} - \frac{2}{\pi} k_F} \left(I_{0F}^{\text{reg}} - \frac{m_N}{2\pi^2} k_F \right) \right]^n \\ &= \sum_{n=0}^{\infty} G^{[n]}(p, P, k_F), \end{aligned} \quad (\text{A41})$$

where $G^{[n]}$ refers to the n -th term contribution in this expansion, which in turn can be rewritten as

$$\begin{aligned} G^{[n]}(p, P, k_F) &= \\ &G^{[0]}(k_F) \left[G^{[0]}(k_F) \left(I_{0F}^{\text{reg}} - \frac{m_N}{2\pi^2} k_F \right) \right]^n. \end{aligned} \quad (\text{A42})$$

By averaging the expansion of the G-matrix over states in the Fermi sea, one obtains the corresponding expansion for the energy per nucleon

$$\frac{E}{A} = \sum_{n=0}^{\infty} \frac{E^{[n]}}{A}. \quad (\text{A43})$$

Then a direct calculation shows:

$$\begin{aligned} \frac{E^{[1]}}{E^{[0]}} &= \frac{k_F}{\frac{1}{a_0} - \frac{2}{\pi} k_F} \left(\frac{4 + 12 \log 2}{35\pi} \right) \\ &= \frac{k_F}{\frac{1}{a_0} - \frac{2}{\pi} k_F} h_F(0), \end{aligned} \quad (\text{A44})$$

where in the second line the numerical factor is written in terms of the function $h_F(x)$ that appeared in Eq. (62).

This expansion can also be mapped into the perturbative expansion of the G-matrix in powers of the in-medium coupling C_{0F} :

$$G = C_{0F}(\Lambda) + C_{0F}^2(\Lambda) I_{0F}(p, P, k_F; \Lambda) + \dots, \quad (\text{A45})$$

though the terms of this expansion are not cutoff independent. For achieving a renormalized expansion one has to expand first the coupling C_{0F} in inverse powers of $(\frac{1}{a_0} - \frac{2}{\pi} k_F)$. For cutoff regularization this yields

$$\begin{aligned} \frac{1}{C_{0F}(\Lambda)} &= \frac{m_N}{4\pi} \left(\frac{1}{a_0} - \frac{2}{\pi} k_F - \frac{4\pi}{m_N} I_{0F}(0, 0, k_F; \Lambda) \right) \\ &= \frac{1}{C_{0F}^{[0]}} - I_{0F}(0, 0, k_F; \Lambda), \end{aligned} \quad (\text{A46})$$

from which one obtains the infrared expansion:

$$\begin{aligned} G(p, P, k_F; \Lambda) &= C_{0F}^{[0]} \\ &\left[1 + C_{0F}^{[0]} (I_{0F}(p, P, k_F; \Lambda) - I_{0F}(0, 0, k_F; \Lambda)) \right. \\ &\quad \left. + \dots \right], \end{aligned} \quad (\text{A47})$$

where the dots indicate the continuation of the geometric expansion. In this case (i.e. with a finite cutoff), the relative size of the first loop correction is

$$\frac{E^{[1]}}{E^{[0]}} = \frac{k_F}{\frac{1}{a_0} - \frac{2}{\pi} k_F} h_F\left(\frac{k_F}{\Lambda}\right), \quad (\text{A48})$$

with the function h_F defined as

$$\begin{aligned} h_F\left(\frac{k_F}{\Lambda}\right) &= \frac{1}{(2\pi^2)} \frac{9}{k_F^7} \\ &\times \frac{4\pi}{m_N} \int_{k_1, k_2 < k_F} \frac{d^3 \vec{k}_1}{(2\pi)^3} \frac{d^3 \vec{k}_2}{(2\pi)^3} \\ &\left[I_{0F}(p, P, k_F; \Lambda) - I_{0F}(0, 0, k_F; \Lambda) \right]. \end{aligned} \quad (\text{A49})$$

In general the closed-form evaluation of this integral is not possible except in a few particular cases. For instance, for a sharp cutoff regulator and a cutoff $\Lambda > 2k_F$ one has

$$\begin{aligned} h_F^{\text{SC}}(x) &= -\frac{2}{35\pi x^7} \left[30x^2 + 99x^4 + 17x^6 - 2x^7 \right. \\ &\quad \left. + 6x^3 (3x^4 - 35) \operatorname{atanh}(x) - 6x^7 \log 2 \right. \\ &\quad \left. + (30 - 126x^2) \log(1 - x^2) \right] \quad (\text{for } x < 1/2), \end{aligned} \quad (\text{A50})$$

while for softer cutoffs the form of h_F^{SC} becomes considerably more involved.

It is not difficult to check that the $\Lambda \rightarrow \infty$ limit of h_F is regulator-independent for separable regulators. This follows from the relation

$$\begin{aligned} \lim_{\Lambda \rightarrow \infty} (I_{0F}(p, P, k_F; \Lambda) - I_{0F}(0, 0, k_F; \Lambda)) \\ = I_{0F}^{\text{reg}}(p, P, k_F) - \frac{m_N}{2\pi^2} k_F \end{aligned} \quad (\text{A51})$$

which is a consequence of Eq. (A15) and

$$\begin{aligned} I_{0F}(0, 0, k_F; \Lambda) &= -\frac{m_N}{2\pi^2} \int_{k_F}^{\infty} f^2\left(\frac{q}{\Lambda}\right) dq \\ &= \frac{m_N}{2\pi^2} \int_0^{k_F} f^2\left(\frac{q}{\Lambda}\right) dq - \frac{m_N}{4\pi} c_r \Lambda. \end{aligned} \quad (\text{A52})$$

Then by averaging over the states within the Fermi sea $h_F(0)$ is recovered.

Appendix B: Loop integrals in the medium

Here I briefly explain how to calculate the loop integrals that are required for the order-by-order renormalization of the EOS, as discussed in Section III. The evaluation of these integrals is necessary for deriving the $k^* - k$ scaling on which the power counting for nuclear matter is based.

For a contact-range theory at tree level the potential energy per nucleon is given by

$$\begin{aligned} \frac{E}{A} &= \frac{1}{2} \left(1 - \frac{1}{g}\right) \rho \\ &\times \left[C_0 + \lambda_2 C_2 \left(\frac{\rho}{g}\right)^{2/3} + \lambda_4 C_4 \left(\frac{\rho}{g}\right)^{4/3} + \dots \right], \end{aligned} \quad (\text{B1})$$

with λ_{2n} a number that depends on the choice of representation of the contact-range potential. For density-dependent couplings this numerical factor is always equal to one ($\lambda_{2n} = 1$), while for energy- and momentum-dependent couplings it is

$$\lambda_{2n} = \frac{18}{(n+1)(n+2)(2n+1)}. \quad (\text{B2})$$

The first loop correction can be schematically written as

$$\begin{aligned} \frac{\delta E}{A} &= \frac{1}{2} \left(1 - \frac{1}{g}\right) \rho \\ &\times \left(\frac{g}{\rho}\right)^2 \left[C_0^2 I_{0F}(k_F; \Lambda) + 2 C_0 C_2 I_{2F}(k_F; \Lambda) + \right. \\ &\quad \left. C_2^2 I_{4F}^{(a)}(k_F; \Lambda) + 2 C_0 C_4 I_{4F}^{(b)}(k_F; \Lambda) + \dots \right], \end{aligned} \quad (\text{B3})$$

where the evaluation of the loop integrals depends on the chosen regularization method and representation of the contact-range potential. In what follows the integrals will be regularized in PDS, which generates relatively simple expressions.

1. Lowest order contact

The loop integral corresponding to the first iteration of C_0 is relatively easy to calculate: one begins with I_{0F} as originally calculated in Eqs. (A10-A13) and averages it for states within the Fermi sea

$$\begin{aligned} I_{0F}(k_F; \Lambda) &= \\ &\int_{k_1 < k_F} \frac{d^3 \vec{k}_1}{(2\pi)^3} \int_{k_2 < k_F} \frac{d^3 \vec{k}_2}{(2\pi)^3} I_{0F}(p, P, k_F; \Lambda), \end{aligned} \quad (\text{B4})$$

where the notation I_{0F} refers either to the loop integral or its average, with the distinction lying in the variables on which it depends.

For its evaluation, one performs a change of variables from the momenta of particles 1 and 2 to the total and relative momentum of the two particle system. That is, the integral for states within the Fermi sea is rewritten

as

$$\begin{aligned} &\int_{k_1 < k_F} \frac{d^3 \vec{k}_1}{(2\pi)^3} \int_{k_2 < k_F} \frac{d^3 \vec{k}_2}{(2\pi)^3} = \\ &\int_0^{2k_F} \frac{P^2 dP}{2\pi^2} \int_0^{\sqrt{k_F^2 - P^2/4}} \frac{p^2 dp}{2\pi^2} \times \\ &\int \frac{d^2 \hat{p}}{4\pi} \theta(k_F - k_1) \theta(k_F - k_2). \end{aligned} \quad (\text{B5})$$

After doing the angular part, the loop integral further simplifies to

$$\begin{aligned} I_{0F}(k_F; \Lambda) &= \\ &\int_0^{2k_F} \frac{P^2 dP}{2\pi^2} \left[\int_0^{k_F - P/2} \frac{p^2 dp}{2\pi^2} + \right. \\ &\quad \left. \int_{k_F - P/2}^{\sqrt{k_F^2 - P^2/4}} \frac{p^2 dp}{2\pi^2} \frac{k_F^2 - (P^2/4 + p^2)}{Pp} \right] \times \\ &\quad I_{0F}(p, P, k_F; \Lambda). \end{aligned} \quad (\text{B6})$$

Following Eqs. (A10) and (A11), the integral can be separated into a diverging and regular component

$$I_{0F}(k_F; \Lambda) = -\frac{1}{(2\pi^2)^2} \frac{m_N}{36\pi} \Lambda k_F^6 + I_{0F}^{\text{reg}}(k_F), \quad (\text{B7})$$

where the regular piece may be further subdivided into

$$I_{0F}^{\text{reg}}(k_F) = I_{0Fa}(k_F) + I_{0Fb}(k_F). \quad (\text{B8})$$

Their explicit evaluation yields

$$I_{0Fa}(k_F) = -\frac{1}{(2\pi^2)^2} \frac{8 m_N}{315 \pi^2} k_F^7, \quad (\text{B9})$$

$$I_{0Fb}(k_F) = -\frac{1}{(2\pi^2)^2} \frac{m_N}{630 \pi^2} (-49 + 6 \log 2) k_F^7, \quad (\text{B10})$$

where by including them in Eqs. (B8) and (B7), one recovers the result of Eq. (97) for $I_{0F}(k_F; \Lambda)$.

2. Higher order contacts

As previously discussed, the loop correction to the energy per nucleon can be written as

$$\frac{\delta E}{A} \propto 2 C_0 C_2 I_{2F} + C_2^2 I_{4F}^{(a)} + 2 C_0 C_4 I_{4F}^{(b)} + \dots \quad (\text{B11})$$

For the density- and energy-dependent representations, the integrals $I_{4F}^{(a)}$ and $I_{4F}^{(b)}$ are identical and the correction simplifies to

$$\frac{\delta E}{A} \propto 2 C_0 C_2 I_{2F} + (C_2^2 + 2 C_0 C_4) I_{4F} + \dots \quad (\text{B12})$$

Meanwhile, for the momentum-dependent representation it is convenient to rewrite the correction as

$$\frac{\delta E}{A} \propto 2 C_0 C_2 I_{2F}(k_F; \Lambda) + (C_2^2 + 2 C_0 C_4) I_{4F}(k_F; \Lambda) + (C_2^2 - 2 C_0 C_4) \bar{I}_{4F}(k_F), \quad (\text{B13})$$

with $I_{4F} = (I_{4F}^{(a)} + I_{4F}^{(b)})/2$ and $\bar{I}_{4F} = (I_{4F}^{(a)} - I_{4F}^{(b)})/2$, where in PDS \bar{I}_{4F} is independent of the regularization scale Λ .

For the density-dependent representation the k_F dependence factorizes and the loop integrals are trivial

$$I_{2F}(k_F; \Lambda) = k_F^2 I_{0F}(k_F; \Lambda), \quad (\text{B14})$$

$$I_{4F}(k_F; \Lambda) = k_F^4 I_{0F}(k_F; \Lambda), \quad (\text{B15})$$

where this pattern extends to higher orders.

For the energy dependent representation, before averaging in the Fermi sea the loop integrals are still trivial and given by

$$I_{2F}(p, P, k_F; \Lambda) = p^2 I_{0F}(p, P, k_F; \Lambda), \quad (\text{B16})$$

$$I_{4F}(p, P, k_F; \Lambda) = p^4 I_{0F}(p, P, k_F; \Lambda). \quad (\text{B17})$$

The averaging leads instead to

$$I_{2F}(k_F; \Lambda) = -\frac{1}{(2\pi^2)^2} \left[\frac{m_N}{120\pi} \Lambda k_F^8 + \frac{m_N}{45360\pi^2} (-632 + 196 \log 2) k_F^9 \right], \quad (\text{B18})$$

$$I_{4F}(k_F; \Lambda) = -\frac{1}{(2\pi^2)^2} \left[\frac{m_N}{280\pi} \Lambda k_F^{10} + \frac{m_N}{249480\pi^2} (-1337 + 564 \log 2) k_F^{11} \right]. \quad (\text{B19})$$

Here it is interesting to notice that the divergent part is λ_{2n} times larger than the corresponding one in the density-dependent representation (with the λ_{2n} coefficients defined in Eq. (B2)).

For the momentum dependent representation it is convenient to define the family of loop integrals

$$I_F^{(2n, 2m)}(p, P, k_F; \Lambda) = p^{2n} \int_{\Lambda} \frac{d^3 q}{(2\pi)^3} q^{2m} \frac{\theta(q_1 - k_F) \theta(q_2 - k_F)}{E - \frac{q^2}{m_N}}, \quad (\text{B20})$$

$$I_F^{(2n, 2m)}(k_F; \Lambda) = \int_{k_1, k_2 < k_F} \frac{d^3 \vec{k}_1}{(2\pi)^3} \frac{d^3 \vec{k}_2}{(2\pi)^3} I_F^{(2n, 2m)}(p, P, k_F; \Lambda). \quad (\text{B21})$$

Note that $I_F^{(2,0)}(k_F; \Lambda)$ and $I_F^{(4,0)}(k_F; \Lambda)$ are simply the energy-dependent loop integrals already calculated in Eqs. (B18) and (B19), respectively. The other three loop

integrals of interest are

$$I_F^{(0,2)}(k_F; \Lambda) = -\frac{1}{(2\pi^2)^2} \left[\frac{m_N}{120\pi} \Lambda k_F^8 + \frac{m_N}{45360\pi^2} (-2040 + 196 \log 2) k_F^9 \right], \quad (\text{B22})$$

$$I_F^{(2,2)}(k_F; \Lambda) = -\frac{1}{(2\pi^2)^2} \left[\frac{m_N}{280\pi} \Lambda k_F^{10} + \frac{m_N}{249480\pi^2} (-3557 + 564 \log 2) k_F^{11} \right], \quad (\text{B23})$$

$$I_F^{(0,4)}(k_F; \Lambda) = -\frac{1}{(2\pi^2)^2} \left[\frac{m_N}{280\pi} \Lambda k_F^{10} + \frac{m_N}{249480\pi^2} (-11321 + 564 \log 2) k_F^{11} \right]. \quad (\text{B24})$$

One can now calculate I_{2F} , I_{4F} and \bar{I}_{4F} in terms of the previous integrals as

$$I_{2F}(k_F; \Lambda) = \frac{1}{2} I_F^{(2,0)}(k_F; \Lambda) + \frac{1}{2} I_F^{(0,2)}(k_F; \Lambda), \quad (\text{B25})$$

$$I_{4F}(k_F; \Lambda) = \frac{3}{8} I_F^{(4,0)}(k_F; \Lambda) + \frac{1}{4} I_F^{(2,2)}(k_F; \Lambda) + \frac{3}{8} I_F^{(0,4)}(k_F; \Lambda), \quad (\text{B26})$$

$$\bar{I}_{4F}(k_F; \Lambda) = -\frac{1}{8} I_F^{(4,0)}(k_F; \Lambda) + \frac{1}{4} I_F^{(2,2)}(k_F; \Lambda) - \frac{1}{8} I_F^{(0,4)}(k_F; \Lambda), \quad (\text{B27})$$

where their explicit evaluation yields

$$I_{2F}(k_F; \Lambda) = -\frac{1}{(2\pi^2)^2} \left[\frac{m_N}{120\pi} \Lambda k_F^8 + \frac{m_N}{45360\pi^2} (-1336 + 196 \log 2) k_F^9 \right], \quad (\text{B28})$$

$$I_{4F}(k_F; \Lambda) = -\frac{1}{(2\pi^2)^2} \left[\frac{m_N}{280\pi} \Lambda k_F^{10} + \frac{m_N}{249480\pi^2} (-5636 + 564 \log 2) k_F^{11} \right], \quad (\text{B29})$$

$$\bar{I}_{4F}(k_F) = -\frac{1}{(2\pi^2)^2} \frac{693 m_N}{249480\pi^2} k_F^{11}. \quad (\text{B30})$$

Before finishing, it is interesting to notice that the momentum dependent representation of the contact-range potential is ambiguous for operators with four derivatives or more. That is, there are multiple on-shell equivalent operators. In the case of C_4 the two options are

$$C_4 \frac{(p^2 + p'^2)}{2} \quad \text{or} \quad C_4 p^2 p'^2, \quad (\text{B31})$$

where for the second operator choice the loop integrals

read

$$I'_{4F}(k_F; \Lambda) = -\frac{1}{(2\pi^2)^2} \left[\frac{m_N}{280\pi} \Lambda k_F^{10} + \frac{m_N}{249480\pi^2} (-4250 + 564 \log 2) k_F^{11} \right], \quad (\text{B32})$$

$$\bar{I}'_{4F}(k_F) = -\frac{1}{(2\pi^2)^2} \frac{(-693)m_N}{249480\pi^2} k_F^{11}, \quad (\text{B33})$$

which are labeled with a prima to distinguish them from the integrals with the first choice, Eqs. (B29) and (B30).

Appendix C: Power counting of the compensating terms

This Appendix explains how to derive the power counting of the lowest order contact-range couplings within the formalism of Section IV. In it power counting is intimately intertwined with the power-law behavior of the reduced wave function at short distances, which determines the scaling of the contributions to the K- and G-matrices from physics at distances below the (r-space) cutoff R_c :

$$\begin{aligned} K(p) \Big|_{r < R_c} &= 4\pi \int_0^{R_c} dr V(r) \frac{\sin pr}{p} u_p(r), \\ G(p, P, k_F) \Big|_{r < R_c} &= 4\pi \int_0^{R_c} dr V(r) \frac{\sin pr}{p} u_{p,P}(r; k_F). \end{aligned} \quad (\text{C1})$$

The arguments are identical in both cases and, for simplicity, only the K-matrix will be discussed in detail.

If the two-body potential V is regular, there will be a regular and irregular solution, where in the regular case

$$u_p^{\text{reg}}(r) = \mathcal{N} [r + \mathcal{O}(r^2)], \quad (\text{C2})$$

with \mathcal{N} a normalization constant that does not depend on the light scales of the system, while in the irregular case

$$u_p^{\text{irr}}(r) = \mathcal{N}(Q) [1 + \mathcal{O}(r)], \quad (\text{C3})$$

where the normalization constant is now a function of the light scales of the system. In this latter case if the range of the potential V is zero then a direct comparison with the expected behavior of the reduced wave function for this type of potential (that is, $u_p(r) = r - a_0$) yields $\mathcal{N} = -a_0$, with a_0 the scattering length. If the range of the potential is short (but not zero) then its effect on the normalization constant is not necessarily trivial, though it is sensible to assume

$$\mathcal{N}(Q) \propto \frac{1}{Q}, \quad (\text{C4})$$

just from its dimensionality alone.

From the previous arguments, in the regular case the zero momentum limit of the $r < R_c$ contribution to the K-matrix is

$$v_0^{\text{reg}}(R_c) = 4\pi \mathcal{N} \int_0^{R_c} dr V(r) [r^2 + \mathcal{O}(r^3)], \quad (\text{C5})$$

while in the irregular one it is:

$$v_0^{\text{irr}}(R_c) = 4\pi \mathcal{N}(Q) \int_0^{R_c} dr V(r) [r + \mathcal{O}(r^2)]. \quad (\text{C6})$$

Provided the potential V does not have a long-range component, the only quantity containing a light scale in this integral is the normalization constant. In particular, if the potential scales as

$$V(r) \propto M f(Mr), \quad (\text{C7})$$

with $f(x) \rightarrow 0$ for $x \gg 1$ (to ensure a short-range potential) and $f(x) \rightarrow f_0$ finite for $x \rightarrow 0$ (to simplify the analysis), one readily finds that v_0 scales as

$$v_0^{\text{reg}}(R_c) \propto \mathcal{N} M R_c^3, \quad (\text{C8})$$

$$v_0^{\text{irr}}(R_c) \propto \mathcal{N}(Q) M R_c^2. \quad (\text{C9})$$

From the condition that the potential is short-ranged ($V(r) \sim 0$ for $Mr \gg 1$), this quantity saturates at $M R_c \sim 1$

$$\int_0^{R_c \gg 1/M} dr V(r) r^\alpha \approx \int_0^{R_c \sim 1/M} dr V(r) r^\alpha, \quad (\text{C10})$$

where α is an exponent ($\alpha = 1, 2$ for the irregular and regular cases, respectively). Thus one arrives at

$$v_0^{\text{reg}}(R_c \gtrsim \frac{1}{M}) \propto \frac{1}{M^2}, \quad (\text{C11})$$

$$v_0^{\text{irr}}(R_c \gtrsim \frac{1}{M}) \propto \frac{1}{M Q}. \quad (\text{C12})$$

If one now matches these coefficients to a contact-range coupling, with a delta-shell regulator at $r = R_c$ (with $M R_c \lesssim 1$):

$$C_0^{\text{reg}}(R_c) \propto \frac{1}{M^2} \quad \text{and} \quad C_0^{\text{irr}}(R_c) \propto \frac{R_c}{M}, \quad (\text{C13})$$

then, by evolving into the infrared ($Q R_c \sim 1$), one recovers the expected power counting for C_0^{irr} .

It is important to notice at this point that the previous power counting argument is non-perturbative, and thus different in character to the perturbative arguments commonly used in the literature. Thus the previous argument can only reliably explain the infrared enhancement of the LO coupling, which is non-perturbative. If applied to the subleading couplings, it arrives to the conclusion that

$$C_{2n}(R_c) \sim C_0(R_c). \quad (\text{C14})$$

Though correct in the regular case, for the irregular solution this leads to the same $1/Q$ enhancement as with C_0 , instead of the usual $1/Q^2$ enhancement. That is, the non-perturbative argument misses part of the infrared enhancement of the subleading (i.e. perturbative) couplings.

This mismatch can be easily solved by considering the expansion of the potential into a LO or non-perturbative part and a subleading or perturbative correction

$$V = V_{\text{LO}} + \delta V. \quad (\text{C15})$$

This entails a similar separation for the K-matrix and reduced wave function

$$K = K_{\text{LO}} + \delta K, \quad (\text{C16})$$

$$u_q = u_q^{\text{LO}} + \delta u_q, \quad (\text{C17})$$

in which case the subleading correction to the K-matrix reads

$$\begin{aligned} \delta K(q) &= 4\pi \int_0^\infty dr \delta V(r) u_q^{\text{LO}}(r) u_q(r) \\ &= 4\pi \int_0^\infty dr \delta V(r) [u_q^{\text{LO}}(r)]^2 + \mathcal{O}((\delta V)^2), \end{aligned} \quad (\text{C18})$$

as can be deduced from distorted-wave perturbation theory. What changes now is that the (non-free) reduced wave function appears squared, thus reproducing the RG arguments of Ref. [34]. If one integrates out again the short-range physics, the result is that the coefficients δv_0 will be now enhanced by a \mathcal{N}^2 factor,

$$\delta v_0^{\text{reg}}(R_c) \propto \mathcal{N}^2 M R_c^3, \quad (\text{C19})$$

$$\delta v_0^{\text{irr}}(R_c) \propto \mathcal{N}^2(Q) M R_c, \quad (\text{C20})$$

leading to

$$\delta v_0^{\text{reg}}(R_c \gtrsim \frac{1}{M}) \propto \frac{1}{M^2}, \quad (\text{C21})$$

$$\delta v_0^{\text{irr}}(R_c \gtrsim \frac{1}{M}) \propto \frac{1}{Q^2}, \quad (\text{C22})$$

plus identical scalings for the $\delta v_{2n}(R_c) p^{2n}$ contributions. When translated into the RG evolution of the subleading couplings, this results in the usual $1/Q^2$ enhancement in the irregular case.

-
- [1] H. Georgi, *Ann. Rev. Nucl. Part. Sci.* **43**, 209 (1993).
[2] E. Epelbaum, H.-W. Hammer, and U.-G. Meissner, *Rev. Mod. Phys.* **81**, 1773 (2009), arXiv:0811.1338 [nucl-th].
[3] R. Machleidt and D. Entem, *Phys.Rept.* **503**, 1 (2011), arXiv:1105.2919 [nucl-th].
[4] H.-W. Hammer, S. König, and U. van Kolck, *Rev. Mod. Phys.* **92**, 025004 (2020), arXiv:1906.12122 [nucl-th].
[5] U. van Kolck, *Front. in Phys.* **8**, 79 (2020), arXiv:2003.06721 [nucl-th].
[6] R. Machleidt and F. Sammarruca, *Prog. Part. Nucl. Phys.* **137**, 104117 (2024), arXiv:2402.14032 [nucl-th].
[7] S. R. Beane, W. Detmold, K. Orginos, and M. J. Savage, *Prog. Part. Nucl. Phys.* **66**, 1 (2011), arXiv:1004.2935 [hep-lat].
[8] S. Aoki, T. Doi, T. Hatsuda, Y. Ikeda, T. Inoue, N. Ishii, K. Murano, H. Nemura, and K. Sasaki (HAL QCD), *PTEP* **2012**, 01A105 (2012), arXiv:1206.5088 [hep-lat].
[9] M. C. Birse, J. A. McGovern, and K. G. Richardson, *Phys. Lett.* **B464**, 169 (1999), hep-ph/9807302.
[10] T. Barford and M. C. Birse, *Phys. Rev.* **C67**, 064006 (2003), arXiv:hep-ph/0206146.
[11] T. Skyrme, *Nucl. Phys.* **9**, 615 (1959).
[12] J. Decharge and D. Gogny, *Phys. Rev. C* **21**, 1568 (1980).
[13] T. Duguet, *Lect. Notes Phys.* **879**, 293 (2014), arXiv:1309.0440 [nucl-th].
[14] M. Grasso, *Prog. Part. Nucl. Phys.* **106**, 256 (2019), arXiv:1811.01039 [nucl-th].
[15] G. Colò, *Adv. Phys. X* **5**, Article: 1740061 (2020).
[16] R. J. Furnstahl, *Lect. Notes Phys.* **852**, 133 (2012), arXiv:nucl-th/0702040.
[17] J. E. Drut, R. J. Furnstahl, and L. Platter, *Prog. Part. Nucl. Phys.* **64**, 120 (2010), arXiv:0906.1463 [nucl-th].
[18] R. J. Furnstahl, *Eur. Phys. J. A* **56**, 85 (2020), arXiv:1906.00833 [nucl-th].
[19] N. Kaiser, *J. Phys. G* **42**, 095111 (2015), arXiv:1505.07095 [nucl-th].
[20] D. Lacroix, *Phys. Rev. A* **94**, 043614 (2016), arXiv:1608.08411 [nucl-th].
[21] C. J. Yang, M. Grasso, K. Moghrabi, and U. van Kolck, *Phys. Rev. C* **95**, 054325 (2017), arXiv:1312.5949 [nucl-th].
[22] C. J. Yang, M. Grasso, X. Roca-Maza, G. Colò, and K. Moghrabi, *Phys. Rev. C* **94**, 034311 (2016), arXiv:1604.06278 [nucl-th].
[23] C. J. Yang, M. Grasso, and D. Lacroix, *Phys. Rev. C* **96**, 034318 (2017), arXiv:1706.00258 [nucl-th].
[24] S. Burrello, M. Grasso, and C.-J. Yang, *Phys. Lett. B* **811**, 135938 (2020), arXiv:2010.12339 [nucl-th].
[25] C. J. Yang, W. G. Jiang, S. Burrello, and M. Grasso, *Phys. Rev. C* **106**, L011305 (2022), arXiv:2110.01959 [nucl-th].
[26] B. Gebremariam, S. K. Bogner, and T. Duguet, *Nucl. Phys. A* **851**, 17 (2011), arXiv:1003.5210 [nucl-th].
[27] R. Navarro Pérez, N. Schunck, A. Dyhdalo, R. J. Furnstahl, and S. K. Bogner, *Phys. Rev. C* **97**, 054304 (2018), arXiv:1801.08615 [nucl-th].
[28] A. Bulgac, M. M. Forbes, S. Jin, R. Navarro Perez, and N. Schunck, *Phys. Rev. C* **97**, 044313 (2018), arXiv:1708.08771 [nucl-th].
[29] L. Zurek, S. K. Bogner, R. J. Furnstahl, R. Navarro Pérez, N. Schunck, and A. Schwenk, *Phys. Rev. C* **109**, 014319 (2024), arXiv:2307.13568

- [nucl-th].
- [30] K. A. Brueckner and C. A. Levinson, *Phys. Rev.* **97**, 1344 (1955).
- [31] K. A. Brueckner, *Phys. Rev.* **100**, 36 (1955).
- [32] H. A. Bethe and J. Goldstone, *Proc. Roy. Soc.(London)* **A238**, 551 (1957).
- [33] L. C. Gomes, J. D. Walecka, and V. F. Weisskopf, *Annals Phys.* **3**, 241 (1958).
- [34] M. Pavón Valderrama and D. R. Phillips, *Phys. Rev. Lett.* **114**, 082502 (2015), arXiv:1407.0437 [nucl-th].
- [35] G. Dahll, E. Østgaard, and B. Brandow, *Nucl. Phys. A* **124**, 481 (1969).
- [36] R. D. Viollier and J. D. Walecka, *Acta Phys. Polon. B* **8**, 25 (1977).
- [37] I. Ruiz Simo, R. Navarro Pérez, J. E. Amaro, and E. Ruiz Arriola, *Phys. Rev. C* **96**, 054006 (2017), arXiv:1708.00878 [nucl-th].
- [38] B. D. Day, *Rev. Mod. Phys.* **39**, 719 (1967).
- [39] U. van Kolck, *Nucl. Phys.* **A645**, 273 (1999), arXiv:nucl-th/9808007.
- [40] J.-W. Chen, G. Rupak, and M. J. Savage, *Nucl. Phys. A* **653**, 386 (1999), arXiv:nucl-th/9902056.
- [41] C. J. Yang, M. Grasso, and D. Lacroix, *Phys. Rev. C* **94**, 031301 (2016), arXiv:1604.06587 [nucl-th].
- [42] M. Grasso, D. Lacroix, and C. J. Yang, *Phys. Rev. C* **95**, 054327 (2017), arXiv:1704.08510 [nucl-th].
- [43] D. Lacroix, A. Boulet, M. Grasso, and C. J. Yang, *Phys. Rev. C* **95**, 054306 (2017), arXiv:1704.08454 [nucl-th].
- [44] R. J. Furnstahl, J. V. Steele, and N. Tiffessa, *Nucl. Phys. A* **671**, 396 (2000), arXiv:nucl-th/9910048.
- [45] J. V. Steele, (2000), arXiv:nucl-th/0010066.
- [46] T. D. Lee and C. N. Yang, *Phys. Rev.* **105**, 1119 (1957).
- [47] D. B. Kaplan, M. J. Savage, and M. B. Wise, *Phys. Lett.* **B424**, 390 (1998), arXiv:nucl-th/9801034.
- [48] D. B. Kaplan, M. J. Savage, and M. B. Wise, *Nucl. Phys.* **B534**, 329 (1998), arXiv:nucl-th/9802075.
- [49] R. J. Furnstahl, H. W. Hammer, and N. Tiffessa, *Nucl. Phys. A* **689**, 846 (2001), arXiv:nucl-th/0010078.
- [50] N. M. Hugenholz and L. van Hove, *Physica* **24**, 363 (1958).
- [51] A. Nogga, R. G. E. Timmermans, and U. van Kolck, *Phys. Rev.* **C72**, 054006 (2005), nucl-th/0506005.
- [52] M. C. Birse, *Phys. Rev.* **C74**, 014003 (2006), arXiv:nucl-th/0507077.
- [53] M. Valderrama, *Phys.Rev.* **C83**, 024003 (2011), arXiv:0912.0699 [nucl-th].
- [54] M. Pavon Valderrama, *Phys.Rev.* **C84**, 064002 (2011), arXiv:1108.0872 [nucl-th].
- [55] M. Pavon Valderrama, *Phys. Rev. C* **113**, 014001 (2026), arXiv:2510.15789 [nucl-th].
- [56] B. Long and C. Yang, *Phys.Rev.* **C84**, 057001 (2011), published version, arXiv:1108.0985 [nucl-th].
- [57] B. Long and C. J. Yang, *Phys. Rev. C* **85**, 034002 (2012), arXiv:1111.3993 [nucl-th].
- [58] B. Long and C. J. Yang, *Phys. Rev. C* **86**, 024001 (2012), arXiv:1202.4053 [nucl-th].
- [59] H. W. Hammer and R. J. Furnstahl, *Nucl. Phys. A* **678**, 277 (2000), arXiv:nucl-th/0004043.
- [60] E. Ruiz Arriola, *Symmetry* **8**, 42 (2016).
- [61] M. P. Valderrama, *Int. J. Mod. Phys. E* **25**, 1641007 (2016), arXiv:1604.01332 [nucl-th].
- [62] M. Pavon Valderrama, *Eur. Phys. J. A* **55**, 55 (2019), arXiv:1901.10398 [nucl-th].
- [63] M. Pavon Valderrama, (2026), arXiv:2603.01561 [nucl-th].
- [64] L. Contessi, M. Schäfer, and U. van Kolck, *Phys. Rev. A* **109**, 022814 (2024), arXiv:2310.15760 [physics.atm-clus].
- [65] L. Contessi, M. Pavon Valderrama, and U. van Kolck, *Phys. Lett. B* **856**, 138903 (2024), arXiv:2403.16596 [nucl-th].
- [66] L. Contessi, M. Schäfer, A. Gnech, A. Lovato, and U. van Kolck, (2025), arXiv:2505.09299 [nucl-th].
- [67] S. Fleming, T. Mehen, and I. W. Stewart, *Nucl. Phys.* **A677**, 313 (2000), arXiv:nucl-th/9911001 [nucl-th].
- [68] A. Ekström and L. Platter, *Phys. Lett. B* **860**, 139207 (2025), arXiv:2409.08197 [nucl-th].
- [69] J. M. Bub, M. Piarulli, R. J. Furnstahl, S. Pastore, and D. R. Phillips, *Phys. Rev. C* **111**, 034005 (2025), arXiv:2408.02480 [nucl-th].
- [70] R. Furnstahl, N. Klco, D. Phillips, and S. Wesolowski, *Phys. Rev. C* **92**, 024005 (2015), arXiv:1506.01343 [nucl-th].
- [71] J. Melendez, S. Wesolowski, and R. Furnstahl, *Phys. Rev. C* **96**, 024003 (2017), arXiv:1704.03308 [nucl-th].
- [72] P. J. Millican, R. J. Furnstahl, J. A. Melendez, D. R. Phillips, and M. T. Pratola, *Phys. Rev. C* **110**, 044002 (2024), arXiv:2402.13165 [nucl-th].
- [73] P. J. Millican, R. J. Furnstahl, J. A. Melendez, and D. R. Phillips, (2025), arXiv:2508.17558 [nucl-th].
- [74] E. Epelbaum, A. M. Gasparyan, J. Gegelia, and U.-G. Meißner, *Eur. Phys. J. A* **54**, 186 (2018), arXiv:1810.02646 [nucl-th].
- [75] P. F. Bedaque, H. W. Hammer, and U. van Kolck, *Phys. Rev. Lett.* **82**, 463 (1999), arXiv:nucl-th/9809025 [nucl-th].
- [76] P. F. Bedaque, H. W. Hammer, and U. van Kolck, *Nucl. Phys.* **A646**, 444 (1999), nucl-th/9811046.
- [77] P. F. Bedaque, H. W. Hammer, and U. van Kolck, *Nucl. Phys.* **A676**, 357 (2000), nucl-th/9906032.
- [78] B. Bazak, J. Kirscher, S. König, M. Pavón Valderrama, N. Barnea, and U. van Kolck, *Phys. Rev. Lett.* **122**, 143001 (2019), arXiv:1812.00387 [cond-mat.quant-gas].
- [79] M. C. Birse, *PoS CD09*, 078 (2009), arXiv:0909.4641 [nucl-th].
- [80] Y.-H. Song, R. Lazauskas, and U. van Kolck, *Phys. Rev. C* **96**, 024002 (2017), [Erratum: *Phys.Rev.C* 100, 019901 (2019)], arXiv:1612.09090 [nucl-th].
- [81] L. Zuo, W. Chen, D.-Y. Pang, and B. Long, (2026), arXiv:2602.15453 [nucl-th].
- [82] G. A. Baker, *Phys. Rev. C* **60**, 054311 (1999).
- [83] M. Pavon Valderrama and E. R. Arriola, *Phys. Rev.* **C74**, 054001 (2006), arXiv:nucl-th/0506047.
- [84] M. P. Valderrama, *AIP Conf. Proc.* **1322**, 205 (2010), arXiv:1009.6100 [nucl-th].
- [85] M. P. Valderrama, *Phys. Rev. C* **111**, 024003 (2025), arXiv:2112.02076 [nucl-th].
- [86] C. Mishra, A. Ekström, G. Hagen, T. Papenbrock, and L. Platter, *Phys. Rev. C* **106**, 024004 (2022), arXiv:2111.15515 [nucl-th].
- [87] R. Machleidt, P. Liu, D. R. Entem, and E. Ruiz Arriola, *Phys. Rev. C* **81**, 024001 (2010), arXiv:0910.3942 [nucl-th].
- [88] M. Pavón Valderrama, M. Sánchez Sánchez, C. J. Yang, B. Long, J. Carbonell, and U. van Kolck, *Phys. Rev. C* **95**, 054001 (2017), arXiv:1611.10175 [nucl-th].
- [89] D. B. Kaplan, *Phys. Rev. C* **102**, 034004 (2020), arXiv:1905.07485 [nucl-th].
- [90] N. Kaiser, S. Fritsch, and W. Weise, *Nucl. Phys. A* **724**,

47 (2003), arXiv:nucl-th/0212049.

[91] J. W. Holt, N. Kaiser, and W. Weise, *Prog. Part. Nucl. Phys.* **73**, 35 (2013), arXiv:1304.6350 [nucl-th].